AEDC-TR-78-36

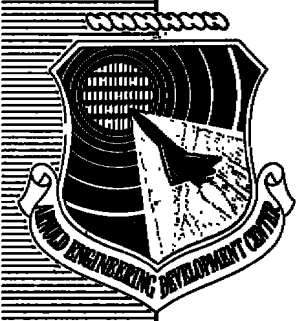

RESEARCH ON ADAPTIVE WALL WIND TUNNELS

R. J. Vidal and J. D. Erickson, Jr.

Calspan Corporation
Buffalo, New York 14221

November 1978

Final Report for Period May 1976 — November 1977

Approved for public release; distribution unlimited.

Prepared for

ARNOLD ENGINEERING DEVELOPMENT CENTER/DOTR
ARNOLD AIR FORCE STATION, TENNESSEE 37389

NOTICES

When U. S. Government drawings, specifications, or other data are used for any purpose other than a definitely related Government procurement operation, the Government thereby incurs no responsibility nor any obligation whatsoever, and the fact that the Government may have formulated, furnished, or in any way supplied the said drawings, specifications, or other data, is not to be regarded by implication or otherwise, or in any manner licensing the holder or any other person or corporation, or conveying any rights or permission to manufacture, use, or sell any patented invention that may in any way be related thereto.

Qualified users may obtain copies of this report from the Defense Documentation Center.

References to named commerical products in this report are not to be considered in any sense as an indorsement of the product by the United States Air Force or the Government.

This final report was submitted by Calspan Corporation, Buffalo, New York 14221 under contract F40600-76-C-0011, with the Arnold Engineering Development Center. Arnold Air Force Station, Tennessee 37389. Dr. M. L. Laster. Mr. Alex Money, and Captain Stephen L. Lamkin, AEDC/DOTR, were the Air Force Technical Representatives.

This report has been reviewed by the Information Office (OI) and is releasable to the National Technical Information Service (NTIS). At NTIS, it will be available to the general public. including foreign nations.

APPROVAL STATEMENT

This report has been reviewed and approved.

Stephen L. Lamkin

STEPHEN L. LAMKIN, Captain, USAF
Project Manager, Research Division
Directorate of Test Engineering

Approved for publication:

FOR THE COMMANDER

Robert W. Crossley

ROBERT W. CROSSLEY, Lt Colonel, USAF
Acting Director of Test Engineering
Deputy for Operations

REPORT DOCUMENTATION PAGE		READ INSTRUCTIONS BEFORE COMPLETING FORM
1. REPORT NUMBER AEDC-TR-78-36	2 GOVT ACCESSION NO.	3 RECIPIENT'S CATALOG NUMBER
4 TITLE (and Subtitle) RESEARCH ON ADAPTIVE WALL WIND TUNNELS		5 TYPE OF REPORT & PERIOD COVERED Final Report - May 1976 - November 1977
		6 PERFORMING ORG. REPORT NUMBER RK-5934-A-1
7 AUTHOR(s) R. J. Vidal and J. C. Erickson, Jr.		8 CONTRACT OR GRANT NUMBER(s)
9 PERFORMING ORGANIZATION NAME AND ADDRESS Calspan Corporation P. O. Box 235 Buffalo, New York 14221		10 PROGRAM ELEMENT, PROJECT, TASK AREA & WORK UNIT NUMBERS Program Element 65807A
11 CONTROLLING OFFICE NAME AND ADDRESS Arnold Engineering Development Center/OIS Air Force Systems Command Arnold Air Force Station, Tennessee 37389		12 REPORT DATE November 1978 13 NUMBER OF PAGES 63
14 MONITORING AGENCY NAME & ADDRESS(if different from Controlling Office)		15 SECURITY CLASS (of this report) UNCLASSIFIED 15a DECLASSIFICATION DOWNGRADING SCHEDULE N/A

16 DISTRIBUTION STATEMENT (of this Report)

Approved for public release; distribution unlimited.

17 DISTRIBUTION STATEMENT (of the abstract entered in Block 20, if different from Report)

18 SUPPLEMENTARY NOTES

Available in DDC

19 KEY WORDS (Continue on reverse side if necessary and identify by block number)

wind tunnels
wall interference
self-correcting
adaptive walls
transonic flow

20 ABSTRACT (Continue on reverse side if necessary and identify by block number)

The objective of this research was to investigate the utility of the Calspan self-correcting wind tunnel for minimizing or eliminating wall interference effects in two-dimensional transonic flows when shock waves from the test model extend to the tunnel walls. This report summarizes the experimental research performed with two-dimensional airfoils in the Calspan self-correcting wind tunnel and the theoretical research accomplished in support of the

DD FORM 1 JAN 73 1473 EDITION OF 1 NOV 65 IS OBSOLETE

20. ABSTRACT (Continued)

experiments. The experiments were performed with airfoil models having 4% and 6% solid blockage. The initial experiments with the 6%-blockage model were devoted to determining a practical mode of operation when shock waves from the model extend to the wall. The most practical mode is to use wall control to obtain the desired distribution of longitudinal velocity components for subcritical walls. The Mach number is then increased and the wall control is readjusted, sequentially, until the desired test condition is achieved. At the high Mach numbers of interest, however, the available wall control was limited locally, and tunnel system changes were required. A method is reported for analyzing self-correcting wind tunnels with porous walls. The analysis treats the auxiliary compressor circuit for wall control, and it provides an approximate method for examining the trade-offs between the compression ratio of the auxiliary compressor, wall porosity, and model size. The most expeditious alternative for extending the operating range was to build and test a 4%-blockage model. The results of iteration experiments with the 4%-blockage model at $M_\infty = 0.85$, $\alpha = 1^o$ are described. They are inconclusive because of flow field fluctuations.

AEDC
Arnold AFS Tenn

SUMMARY

The objective of this research was to investigate the utility of the Calspan self-correcting wind tunnel for minimizing or eliminating wall interference effects in two-dimensional transonic flows when shock waves from the test model extend to the tunnel walls. An adaptive wall wind tunnel can eliminate wall interference effects on a test model by the use of redundant measurements of flow field quantities in the test section and by active control of the flow in the vicinity of the wind tunnel walls to insure that the measured quantities satisfy functional relationships for unconfined flow. There are a number of methods available for exerting control of the flow at the tunnel walls. The Calspan embodiment is a perforated wall test section with a segmented plenum, and control is achieved by adjusting the local flow through the porous walls. Experiments at low transonic Mach numbers wherein the walls are subcritical have demonstrated the validity of the basic concept. The specific objective of this research program was to extend the range of the Calspan tunnel to minimize or eliminate wall interference effects on a two-dimensional lifting airfoil when the walls are supercritical.

This report summarizes the experimental research performed with two-dimensional airfoils in the Calspan self-correcting wind tunnel and the theoretical research accomplished in support of the experiments. The experiments were performed with airfoil models having 4% and 6% solid blockage. The initial experiments with the 6%-blockage model were devoted to determining a practical mode of operation when shock waves from the model extend to the walls. The previously established operational model produced choked flow at and downstream of the model. The most practical mode of operation which resulted is to use wall control to obtain the desired distributions of longitudinal velocity components for subcritical walls. The Mach number is then increased and the wall control is readjusted, suquentially, until the desired test condition is achieved. At the high Mach number of interest, however, the available wall control was limited locally, and the wind tunnel system changes were required.

A method is reported for analyzing and designing self-correcting wind tunnels with porous walls. The analysis treats the auxiliary compressor circuit for wall control, and it provides an approximate method for examining the trade-offs between the compression ratio of the auxiliary compressor, wall porosity, and model size. For the purposes of this research, the most expeditious alternative for extending the operating range was to build and test a 4%-blockage model.

The results of iteration experiments with the 4%-blockage model at $M_\infty = 0.85$, $\alpha = 1°$ are described. They are inconclusive because of flow field fluctuations. Wall control was used to obtain a first approximation to the unconfined flow field, but the shock wave on the lower surface fluctuated over about 15% of the chord. Subsequent attempts to iterate at this test condition did not lead to a steady flow field, and it is concluded that this test condition is not suitable for iteration at this stage of the development.

PREFACE

This report describes the work performed by Calspan Corporation for the Department of the Air Force under Contract No. F40600-76-C-0011. The contractor's report No. RK-5934-A-1 is also used to identify this report. The work was carried out specifically for Headquarters, Arnold Engineering Development Center DOTR, Arnold Air Force Station, Tennessee. Technical Representatives for the Air Force were Dr. M. L. Laster, Mr. Alex Money, and Captain Stephen L. Lampkin.

The investigation was conducted in the Aerodynamic Research Department of Calspan Corporation, Buffalo, New York, and was managed by Mr. Robert J. Vidal. The work was accomplished between May 1976 and November 1977.

The reproducibles used for this report were supplied by the authors, R. J. Vidal and J. C. Erickson, Jr. The authors wish to acknowledge the contributions to the investigation by Professor W. R. Sears of the University of Arizona, a consultant to Calspan, as well as by Calspan personnel Dr. A. Ritter, P. A. Catlin, D. C. Daughtry, and A. F. Gretch.

TABLE OF CONTENTS

LIST OF FIGURES

LIST OF FIGURES (Cont'd)

LIST OF FIGURES (Cont'd)

1.0 INTRODUCTION

Achievement of interference-free wind tunnel data at transonic speeds is a problem of long standing. Current practice generally is to test models which are small enough with respect to the tunnel so that wall interference effects are minimized. Often the interference can be neglected completely. However, recent experience with the extrapolation of tunnel data to full-scale flight conditions of large aircraft has demonstrated the importance of testing larger models to achieve higher Reynolds numbers. Moreover, the high lift requirements of contemporary combat aircraft lead to large flow deflections within the tunnel. The necessity for testing larger models with greater flow deflections than are the current practice can lead to testing beyond the operational bounds for which wall corrections may be ignored.

The question of estimating wall interference corrections for models tested in a transonic tunnel has remained open over the years. The basic idea of interference corrections is deceptive, even in the case of solid wall or open jet wind tunnels, because the interference effects are not distributed uniformly over the test model. The difficulties are compounded in the case of transonic wind tunnels with ventilated test sections because the flow processes at the ventilated walls are complex and cannot be modeled in the simple manner that is desirable for theoretical corrections. The recognition of these deficiencies has led to the general concept of an adaptive-wall or self-correcting wind tunnel.

The basic concept of the self-correcting wind tunnel is documented in the literature.[1,2] Briefly, it is based on the premise that unconfined flow conditions in the working section can be determined by measurements with sensors located in the airstream. The presence of the model produces disturbances in the velocity components, pressure, density, etc., of the uniform stream. In unconfined flow, the values of these disturbance quantities at some control surface locations bear certain functional relationships to one

1. Sears, W.R. "Self-Correcting Wind Tunnels" (The Sixteenth Lanchester Memorial Lecture) The Aeronautical Journal, Vol. 78, No. 758/759, February/March 1974, pp. 80-89.

2. Ferri, A. and Baronti, P. "A Method for Transonic Wind Tunnel Corrections" AIAA Journal, Vol. 11, No. 1, January 1973, pp. 63-66.

another, which are due to the nature of the fluid stream and the very strong condition that it is unconfined at infinity. If one of these quantities is known all along the control surfaces, it defines the flow external to the surfaces so that all the other quantities can be found. Therefore, unconfined flow in the working section of the tunnel is determined by the model configuration together with the condition that the unconfined flow functional relationships are satisfied at the control surfaces. These relationships constitute the statement that the flow is unconfined, so far as the flow about the model is concerned.

In a wind-tunnel experiment, in general, quantities measured at the control surfaces would deviate from these functional relationships because the fluid is not unconfined, and such deviation is a measure of the departure from unconfined flow conditions. If the flow field in the vicinity of the test section walls can be adjusted at will, however, it can be adjusted until the existence of unconfined, free-flight conditions within the tunnel is signaled by the fact that the proper functional relationships exist among the quantities measured at the control surfaces. The self-correcting wind tunnel, then, combines both experimental and theoretical techniques in such a way that each is used to its best advantage for simulating free-flight conditions about a model in a wind tunnel.

A research program has been in progress at the Calspan Corporation since November 1971* to demonstrate, both theoretically and experimentally, that the self-correcting concept can be implemented in two-dimensions.[1,3-6]

*Sponsored by ONR and AFOSR under Contract No. N00014-72-C-0102, with supplemental support by NASA/Langley Research Center; and by ONR and AFOSR under Contract No. N00014-77-C-0052.

3. Erickson, J.C., Jr., and Nenni, J.P. "A Numerical Demonstration of the Establishment of Unconfined-Flow Conditions in a Self-Correcting Wind Tunnel" Calspan Report No. RK-5070-A-1, November 1973.

4. Vidal, R.J., Catlin, P.A. and Chudyk, D.W. "Two-Dimensional Subsonic Experiments with an NACA 0012 Airfoil" Calspan Report No. RK-5070-A-3, December 1973.

5. Vidal, R.J., Erickson, J.C., Jr., and Catlin, P.A. "Experiments With a Self-Correcting Wind Tunnel" AGARD CP No. 174 on Wind Tunnel Design and Testing Techniques, October 1975.

6. Sears, W.R., Vidal, R.J., Erickson, J.C., Jr., and Ritter, A. "Interference-Free Wind-Tunnel Flows by Adaptive-Wall Technology" Journal of Aircraft, Vol. 14, No. 11, November 1977, pp. 1042-1050.

That work has been summarized recently in References 5 and 6. Theoretically, functional relationships for unconfined flow have been established both for subcritical and for supercritical flows at the control surfaces. Computer programs for these relationships have been checked out, and their accuracy has been verified by theoretical examples. In addition, both low-speed flows and transonic flows about an airfoil in a self-correcting wind tunnel test have been simulated numerically to test a proposed iteration technique. This technique converged successfully, and similar tests at subsonic speeds showed that the expected sensor accuracies were consistent with the desired degree of unconfined flow.

Experimentally, a two-dimensional airfoil model with an NACA 0012 section and a 6-inch chord was fabricated and tested in the Calspan Eight-Foot Transonic Wind Tunnel to establish the airfoil characteristics in unconfined flow. Sensor evaluation experiments in the Calspan One-Foot Transonic Wind Tunnel have also been carried out and the self-correcting test section for the One-Foot Tunnel has been designed, fabricated, installed in the wind tunnel circuit and run.

The basis of the design of the Calspan self-correcting wind tunnel is the segmentation of the test section plenum and application of active wall control by blowing or suction in the plenum segments. Calibration experiments in the empty tunnel show that without active wall control, the flow is relatively poor with the Mach number varying by about 20% over the length of the test section. However, active wall control eliminates these poor characteristics and makes the tunnel comparable with existing facilities. The experiments with the 6-inch chord airfoil in the tunnel (6% blockage), and with the tunnel operated to simulate a conventional porous wall wind tunnel, show that there are large wall interference effects on the forces including important shifts in the positions of the shock waves. Typical results obtained by approximating a conventional porous wall wind tunnel show that for the 6%-blockage NACA 0012 airfoil at $M_\infty = 0.725$ and $\alpha = 2°$, the shock wave on the upper airfoil surface is located about 12% of the chord aft of the interference free position. The errors due to wall interference are about 30% in lift, 70% in drag, 60%

in pitching moment. Comparisons with data obtained on the same airfoil in the Eight-Foot tunnel show that active wall control, used in conjunction with our iterative procedure but without complete convergence, largely reproduces the correct shock wave position, eliminates wall interference on lift and drag, and reduces the interference effects on pitching moment to 10%. In view of these results and others,[5-6] we view the iteration experiments in the self-correcting wind tunnel as being basically successful for subcritical walls.

The objective of the investigation reported here was to extend the operational range of the Calspan One-Foot self-correcting wind tunnel to higher Mach number flows for which the locally supersonic regions reach the control surfaces and the tunnel walls. This investigation was complemented in certain instances by work carried out under ONR/AFOSR Contract No. N00014-77-C-0052, as indicated below.

The first experiments at higher Mach numbers are described in Section 2, with principal emphasis on the establishment of operational procedures for setting a desired tunnel flow field. These experiments were made with the 6%-blockage model, and although a procedure was developed it was found that the desired flow field control could not always be achieved at all locations in the test section. This led to a detailed auxiliary compressor circuit analysis, described in Section 3 and carried out jointly with the ONR/AFOSR effort. The results of this analysis are described, and they demonstrate the trade-offs available with self-correcting wind tunnels. This study led to the conclusion that the most efficient method for continuing the present investigation with the existing apparatus would be to use a 4%-blockage model. It was fabricated, and initial experimental results with this model are presented in Section 4. The investigation is summarized in the concluding remarks, Section 5, and details are given in the Appendix of some efforts carried out in support of the experiments, namely probe calibrations, calculation of first approximations to begin the iterations, and improvements to the evaluation procedures for the functional relationships.

2.0 EXPERIMENTS TO ESTABLISH AN OPERATIONAL MODE

The experimental set-up is shown in Fig. 1. The test section is 10-inches wide and 12-inches high, and the airfoil is an NACA 0012 section with a 6-inch chord. Consequently, the solid blockage with this model is 6%. The instrumentation for inferring the two components of the disturbance velocity is partially visible; the two static pressure pipes are mounted approximately 3.93 inches above and below the centerline, and the probes for measuring flow angle (Fig. 2) are 4.5 inches above and below the centerline. These locations were selected to minimize interference effects between the pipes and the probes.

The test conditions selected for the initial experiments were $M_\infty = 0.85$ and the airfoil model at $\alpha = 1^o$. This is an interesting test condition because the data from the Eight-Foot Tunnel tests,[4] shown in Figures 3 and 4, show unusual airfoil characteristics. Figure 3 shows that the lift curve slope is very small at small angles of attack, and Figure 4 shows that both the upper and lower airfoil surfaces are supercritical over about 70% of the chord length. It might be expected that the unusual shock wave formations on the upper and lower surfaces would be sensitive to wall interference effects, and this test condition should provide a severe test of the self-correcting scheme.

We followed our established subcritical-wall procedure in the initial experiments; a theoretical estimate was made for the disturbance velocity components at the control surfaces using Prandtl-Glauert theory (see the Appendix), and wall control was used to set one of these components. These estimates show that the flow at the control surfaces would be slightly supercritical, Figures 5 and 6. The mode of operation that we have been using[5] is to apply wall control simply to establish the desired distributions of longitudinal disturbance velocities at the control surfaces, and it was used here.

The results obtained at the control surfaces are shown in Figures 5 and 6. It can be seen that upstream of the airfoil quarter chord we were able to achieve the desired distributions very closely but were unable to set up the desired distributions downstream of this location. In fact, the flow downstream was supersonic with multiple shock waves extending beyond the control surfaces. The pressure distribution measured on the airfoil is shown in Figure 7. These data are consistent with the flow at the control surfaces and correspond to a local Mach number on the airfoil in excess of 1.30. Comparing the data obtained in the One-Foot Tunnel with those obtained in the Eight-Foot Tunnel, it can be seen that the wall interference effects on the model are sizable, and the largest effect is on the position of the shock waves on the airfoil. Although we have no data beyond $x/c = 0.90$, wall interference has moved the shock somewhere aft of this point.

It is clear from Figures 5 and 6 that the operational mode is not suitable for this test condition, and a number of experiments were performed in an attempt to modify the mode. These included varying the distribution of porosity in the vicinity of the model and reversing the control sequence; i.e., applying blowing instead of suction when supersonic flow was observed. Each of these was partially successful in that we were able to reduce the flow Mach number downstream of the airfoil; however, we were not able to control the entire downstream flow field. An example of this improved control is illustrated in Figures 8 to 10. It can be seen that we were able to produce the desired flow field in the vicinity of the model, but were unable to prevent the flow from accelerating to M = 1.05 at the downstream end of the test section, producing a strong normal shock wave in the diffuser. Figure 10 shows that this improved control modified the airfoil pressure distribution favorably, moving the airfoil shock waves from the trailing edge nearer to the correct positions.

The above method of regaining flow field control is an inefficient approach, as evidenced by the normal shock wave in the diffuser. Consequently, we halted those attempts in favor of two more direct methods. The first is to use wall control to obtain the desired normal velocity components, in

contrast to the present procedure of controlling the longitudinal velocity component. The second is to approach the case of supercritical walls more gradually by establishing control at a lower Mach number and then working up in Mach number.

The next set of experiments was thus designed to investigate these new modes of operation for conditions where the walls are supercritical. The first case was a wholly subcritical one, namely $M_\infty = 0.80$, $\alpha = 1^\circ$. We had run at this test condition previously and had been able to exert the desired wall control to establish the longitudinal components of the disturbance velocity. Here, though, we first used wall control to establish the normal velocity components, and those results are presented in Figures 11-15. Figures 11 and 12 show the Prandtl-Glauert normal velocity distributions we were trying to set as well as the normal velocities that were obtained. It can be seen that we were able to obtain the desired normal velocities upstream of the model, but we were not able to establish all of the desired values in the remainder of the flow field. The source of this difficulty is apparent from the distributions of the longitudinal velocity, Figures 13 and 14. The distributions of the longitudinal velocity upstream of the model are reasonable, but downstream of the model the flow is supersonic, much like the conditions previously observed at $M_\infty = 0.85$, $\alpha = 1^\circ$ in Figures 5 and 6. The schlieren photograph in Figure 15 confirms these observations and also shows that shock waves were produced by the probes near the walls.

The experimental observation that direct control of the normal velocity component is impractical can be explained qualitatively using Prandtl-Glauert theory and linearized supersonic theory. It is recognized that these theories are limited in the vicinity of $M_\infty = 1$, but they illustrate the trends that can be expected. The effects of the model thickness on the flow field becomes increasingly important in the transonic regime and can dominate the lift effects. It can be shown that for a doublet in the Prandtl-Glauert regime, the ratio of the longitudinal velocity component to the normal velocity component is

$$\frac{u}{v} = \frac{x^2 - \beta^2 y^2}{2\beta x(\beta y)} \tag{1}$$

where $\beta = \sqrt{1 - M_\infty^2}$, and x and y are the longitudinal and normal coordinates. At a point along the control surface, x = ky, where k is an arbitrary constant (but not zero), the velocity ratio is

$$\frac{u}{v} = \frac{1}{2}\left[\frac{k}{1 - M_\infty^2} - \frac{1}{k}\right] \tag{2}$$

Consequently in the transonic range, small changes in the normal velocity component, v, correspond to large changes in the longitudinal velocity component, u.

Similarly, in linearized supersonic flow, the ratio of the two velocity components is

$$\frac{u}{v} = -\frac{1}{\sqrt{M_\infty^2 - 1}} \tag{3}$$

and in the transonic range, small changes in the normal velocity component, v, also correspond to large changes in the longitudinal velocity component, u. These arguments, coupled with our experimental experience, make it clear that the best mode of operation still is to use wall control to establish the desired distributions of longitudinal velocity components.

We repeated this test condition, $M_\infty = 0.80$, $\alpha = 1^\circ$, using wall control to establish the desired distributions of the longitudinal disturbance velocity, to check again to see if the desired control could be exerted at these conditions. The results are shown in Figures 16 to 20. It can be seen in Figures 16 and 17 that we were able to establish control over the longitudinal disturbance velocities, and that the corresponding normal velocities, Figures 18 and 19, are in reasonable agreement with the estimates based on Prandtl-Glauert theory. The schlieren photograph, Figure 20, shows that the shock wave is near the correct position, as indicated by the Eight-Foot Tunnel data, and confirms that the control surfaces are subcritical.

We next performed experiments at $M_\infty = 0.85$, $\alpha = 1^\circ$, after introducing the area change in the tunnel diffuser described below in Section 3. The operational mode here was the second approach mentioned above, namely to use wall control to establish the desired distributions of longitudinal disturbance velocities, beginning from the settings at $M_\infty = 0.80$, $\alpha = 1^\circ$. Then the Mach number was increased to 0.85 and the wall controls were readjusted to obtain the desired distributions at the new Mach number. The results of this experiment are shown in Figures 21 to 25. The distributions of the longitudinal velocity, Figures 21 and 22, are in reasonable agreement with the Prandtl-Glauert estimates, particularly upstream and downstream of the model. The differences are probably due to limitations in the theory at this Mach number. The important point, however, is that by means of this mode of operation, we were able to achieve wall control for conditions where the local Mach number at the control surfaces was about 1.05.

The corresponding distributions of normal velocity, shown in Figures 23 and 24, are reasonable in that the distributions are physically plausible. The discrepancies between the data and the Prandtl-Glauert estimates reflect the fact that the flow is not unconfined and hence iterative wall adjustments are required. The schlieren photograph, Figure 25, should be compared with Figure 15, because the latter is representative of the flow field when we were unable to exert the desired control. Figure 25 shows that through wall control we were able to duplicate closely the correct shock wave positions. The shock waves emanating from the flow angle probe provide evidence that the control surfaces were supercritical.

Having achieved some degree of wall control at $M_\infty = 0.85$, $\alpha = 1^\circ$, we normally would have begun iterating toward unconfined flow. However, one of the plenum chambers in the vicinity of the model was at the limit of its control. Consequently, we were not confident that we could achieve the next iterative step so did not proceed. This difficulty led to a detailed analysis of the auxiliary compressor circuit, described in the next Section, to identify the source of this limitation and to indicate the best means for correcting it.

3.0 AUXILIARY CIRCUIT ANALYSIS

Our experience with the self-correcting wind tunnel has shown that the wind tunnel's performance range is limited because we are not always able to effect the desired flow field control at all test conditions. We have modified the auxiliary compressor circuit in order to minimize some extraneous losses and have made measurements to determine if further modifications are warranted. These measurements have been used in conjunction with the analysis below to assess the tunnel's performance.

The auxiliary suction system is shown schematically in Figure 26. The analysis starts with the pressure balance, noting that the compressor has a fixed compression ratio, R_c .

$$p_\infty + \Delta p_d + \Delta p_{BL} = R_c \left[p_\infty + \Delta p_{ff} - \Delta p_w - \Delta p_{VL} \right] \tag{4}$$

where

$$\Delta p_d = p_9 - p_\infty \;,\; \Delta p_{BL} = p_1 - p_9 \;,\; \Delta p_{ff} = p_2 - p_\infty \;,\; \Delta p_w = p_2 - p_2 \;,\; \Delta p_{VL} = p_2 - p_6$$

The available pressure drop across the wall is:

$$\frac{\Delta p_w}{q_\infty} = \frac{2}{\gamma M_\infty^2}\left(1 - \frac{1}{R_c}\right) + \frac{\Delta p_{ff}}{q_\infty} - \frac{\Delta p_{VL}}{q_\infty} - \frac{1}{R_c}\left(\frac{\Delta p_d}{q_\infty} + \frac{\Delta p_{BL}}{q_\infty}\right) \tag{5}$$

The losses in the pipes, Δp_{VL} and Δp_{BL} , are governed by

$$\Delta p = \lambda \frac{L}{d} \rho \bar{u}^2 \;, \quad \lambda = \frac{\text{const.}}{\left(\rho \frac{\bar{u} d}{\mu}\right)^{1/4}}$$

We have found that the volumetric flow through the compressor is essentially invariant for our range of test conditions. Further, one would expect the density in the auxiliary circuit to be a fixed fraction of the test section density. If we neglect the one-fourth power variations, the losses in the pipes will vary as the square of the free-stream velocity, or

$$\frac{\Delta p_{VL}}{q_\infty} = \frac{2C_1}{\gamma M_\infty^2}\left(1 + \frac{\gamma-1}{2} M_\infty^2\right), \quad \frac{\Delta p_{BL}}{q_\infty} = \frac{2C_2}{\gamma M_\infty^2}\left(1 + \frac{\gamma-1}{2} M_\infty^2\right) \quad (6)$$

where the constants C_1 and C_2 are determined experimentally for our circuit. Similarly, it can be shown from the one-dimensional channel-flow equations that the recompression pressure loss varies approximately as

$$\frac{\Delta p_d}{q_\infty} = \frac{2}{\gamma M_\infty^2}\left(C_3 + C_4 M_\infty^2 + C_5 M_\infty^4\right) \quad (7)$$

where the constants C_3, C_4 and C_5 were also determined experimentally for the compressor circuit. The relations in Equations (6) and (7) have been combined with Equation (5) to obtain the following relation for estimating the tunnel performance.

$$\frac{\Delta p_w}{q_\infty} - \frac{\Delta p_{ff}}{q_\infty} = \frac{2}{\gamma M_\infty^2}\left\{1 - \frac{1}{R_c} - \left(1 + \frac{\gamma-1}{2} M_\infty^2\right)\left(C_1 + \frac{C_2}{R_c}\right) - \frac{1}{R_c}\left(C_3 + C_4 M_\infty^2 + C_5 M_\infty^4\right)\right\} \quad (8)$$

We have used Chew's data[7] for the loss characteristics of porous walls and have obtained the empirical correlation shown in Figure 27, namely that the wall loss characteristics vary as

$$\frac{1}{M_\infty}\frac{\Delta p_w}{q_\infty} = K\left(\frac{v}{U_\infty}\right)^2 \quad (9)$$

Chew's data cannot be used directly in estimating losses across a porous wall because those data were determined from measurements of the volumetric flow through the walls. Consequently, they do not account for the amplification effect of the wall boundary layer. We have made measurements of the pressure drop across the wall and the normal velocity component in the inviscid stream

7. Chew, W.L. "Cross-Flow Calibration at Transonic Speeds of Fourteen Perforated Plates with Round Holes and Airflow Parallel to the Plates" AEDC-TR-54-65, July 1955.

for our walls, which have a porosity σ of 22.5%, and have shown that those data correlate within the parameters of Fig. 27 but with a different constant, namely K = 111.

We combined Equations (8) and (9) and used that result to estimate the performance of the present tunnel configuration. The solid curve in Figure 28 shows the maximum normal velocity component that can be obtained, neglecting the model flow field effect, as a function of Mach number for our compressor, R_c = 1.43. Included in Figure 28 is a limiting line corresponding to choked flow through the existing σ = 22.5% walls. We have also calculated the model flow field effect and the normal velocity component required at the model quarterchord, see Figure 28. These estimates are based on Prandtl-Glauert theory for $\alpha = 1^{\circ}$. It can be seen that the available and required wall control are equal at $M_\infty \approx 0.86$. This is in good agreement with our experience where we have found that the wall control is limited somewhere below M_∞ = 0.85. This suggests that the circuit analysis is adequate for our present purposes.

One conclusion from this analysis was that the recompression penalty, Δp_d in Equation (5), could be reduced considerably. This can be accomplished by introducing an area change in the tunnel diffuser at the location where the flow from the auxiliary blower is vented into the tunnel circuit. The best arrangement is to generate sonic flow at that location, so that there would be suction on the blower discharge. Eq. (8) describing the blower circuit performance then becomes

$$\frac{\Delta p_\omega}{q_\infty} - \frac{\Delta p_{ff}}{q_\infty} = \frac{2}{\gamma M_\infty^2}\left\{1 - \frac{1}{R_c} - \left(1 + \frac{\gamma-1}{2} M_\infty^2\right)\left(C_1 + \frac{C_2}{R_c}\right) + \frac{1}{R_c}\left[1 - \left(\frac{1 + \frac{\gamma-1}{2} M_\infty^2}{\frac{\gamma+1}{2}}\right)^{\frac{\gamma}{\gamma-1}}\right]\right\} \quad (10)$$

and when combined with Equation (9) can be used to predict the circuit performance. This is illustrated in Figure 29 along with results for other values of R_c that will be discussed below. This area change modification promises a considerable improvement in the circuit performance at lower Mach numbers, see Figure 28 for comparison, and indicates an increase in the limiting Mach number from 0.85 to 0.90.

We installed such an area change in the tunnel diffuser to produce nearly sonic flow at the location where the blower is vented to the main tunnel circuit, and we made exploratory experiments to assess the wall control. These consisted of setting the longitudinal disturbance velocities predicted by Prandtl-Glauert theory. We were able to exert the desired control at M_∞ = 0.80 and 0.85 (see the previous section), but were not able to exert the desired control at $M_\infty \approx 0.90$. From this we concluded that the disturbance velocities produced by the 6%-blockage model at higher Mach numbers are too large to control with the existing experimental equipment. Four alternatives for alleviating this condition were considered; 1) use of an auxiliary compressor with a higher compression ratio R_c, 2) use of walls with a higher porosity σ, 3) moving the model off the tunnel centerline, and 4) construction and testing of a smaller-chord 0012 airfoil model.

The effect of using an auxiliary compressor with a higher compression ratio can be seen by reference to Fig. 29. There, the maximum available normal velocity that can be obtained without considering the model flow field is given for the additional compression ratios of 2 and 10^7. This figure shows that the best to be expected would be an increase of performance until the limit of choked perforations was reached at all Mach numbers. With the 6%-blockage model, this would enable us to increase the limiting Mach number from 0.90 to about 0.915.

This result leads to examination of the possibility of using test section walls with a porosity σ greater than 22.5%. An assessment was carried out, again using the wall loss characteristics reported by Chew.[7] The data he obtained at M_∞ = 0.90 were correlated in terms of the parameters, $\frac{1}{M_\infty}\frac{\Delta p_w}{q_\infty}$ and $\left(\frac{v}{U_\infty}\right)^2$ for σ values of 5.2%, 11.8%, 22.5%, and 33%. These correlations are presented in Fig. 30 and it can be seen that they are sufficiently accurate for the present purposes. The correlations in Fig. 30

were used to determine the constant, K, in the equation for the wall loss characteristics, Eq. 9, and this constant is plotted as a function of porosity in Fig. 31. As described above, we require a similar curve, but with a different constant. For analysis purposes, we assume that the boundary layer amplification factor is independent of porosity; i.e., we assume that the wall loss characteristics are described by the line through the single Calspan data point in Fig. 31. The tunnel performance estimated with this correlation is presented in Fig. 32 for σ's of 22.5%, 33%, and 50%. It can be seen that an increase in porosity improves the capabilities of wall control at any given Mach number. For example at $M_\infty = 0.85$, an increase in wall porosity from 22.5% to 50% doubles the available v/U_∞. However, this increase only changes the limiting Mach number from 0.90 to 0.92. Furthermore, additional effort is required to assess the effect of increased wall porosity on the wave cancellation properties for the adaptive-wall application.

It does appear that a combination of a new auxiliary compressor with higher R_c and walls with higher σ might hold promise of improving the system characteristics. However, the cost and time delays inherent in this implementation did not seem justified in order to make timely progress. The third alternative, testing the model off the test section centerline, was considered in some detail but was not implemented because it is not readily accomplished with our experimental apparatus. As shown in Figure 1, the model is supported on shafts and bearings extending through glass windows, and it would be necessary to drill new holes.

We concluded, therefore, that the most expeditious method for investigating the performance of the self-correcting wind tunnel with supercritical walls is to continue with the present wind tunnel configuration, 22.5% porous walls, and to use a slightly smaller 4%-blockage model. It should be emphasized that we do not regard either 6% blockage or 4% blockage as upper limits on model size for a self-correcting wind tunnel. The circuit analysis cited above indicates that the tunnel performance can be improved by sizing the wall characteristics, the auxiliary pumping system, the model, and the tunnel circuit in keeping with specific objectives. We elected to

use a smaller model as the alternative that would allow timely investigation of the tunnel characteristics with supercritical walls. Before leaving the circuit analysis, it should be noted that it does form a sound basis for the design and future development of advanced self-correcting wind tunnels. It provides a rational method for sizing models, test sections, and auxiliary compressor circuits, and in fact, it could serve as a basis for working charts to define the operational range for any given self-correcting facility.

4.0 EXPERIMENTS WITH A 4%-BLOCKAGE MODEL

An airfoil model with an NACA 0012 section and a 4-inch chord (4% blockage) was constructed and is being tested to investigate the self-correcting wind tunnel with supercritical control surfaces. The model has a row of pressure orifices along its centerline on the upper and lower surfaces, but there are no provisions for measuring the forces and moment directly. The first experiments were performed with the model nominally at 1^{o} angle of attack and with a free-stream Mach number of 0.85. As noted in Section 2, this test condition was selected because the Eight-Foot Tunnel results, Figs. 3 and 4, show that the lift curve slope is very small due to the unusual shock wave locations on the upper and lower surfaces.

Several attempts were made to iterate this particular case. The wall control was adequate at all times, but we were unable to establish the desired velocity distributions beyond the first approximation. We could exert the desired control, sequentially, proceeding from the beginning of the test section to the model. However, subsequent small adjustments immediately downstream of the model produced a sudden change in the flow field in the vicinity of the model that called for new adjustments to the entire flow field.

The basic source of the difficulty is illustrated by the schlieren photographs in Fig. 33. These were taken at different times after the first approximation had been established, and they show that the shock wave positions were fluctuating. The shock waves tended to form correctly, according to the Eight-Foot Tunnel data, at the rear position, but then moved forward and returned to the rear position with a period of about 10 seconds. The excursions were larger on the lower surface, covering about 15% of the chord.

The results from the Eight-Foot Wind Tunnel were re-examined to see if any indication of these fluctuations was present in those experiments. Duplicate data had been taken in those experiments, and a comparison of the pressure data showed excellent repeatability. Consequently, it appears that

this test condition was steady in an essentially unconfined flow, and so the residual wall interference in the One-Foot Tunnel, even after setting the first approximation, may be sufficient to produce the observed fluctuations.

It is clear that these shock wave fluctuations have unnecessarily complicated the basic objective of investigating the self-correcting wind tunnel under conditions where the control surfaces are supercritical. Consequently, investigations in the immediate future will not use this test condition, but will be made with test conditions where the flow field is steady. Exploratory experiments have indicated that stable, supercritical test conditions can be attained.

5.0 CONCLUDING REMARKS

The purpose of this research has been to extend the operating range of the Calspan self-correcting wind tunnel to conditions where the control surfaces and the tunnel walls are supercritical. The early experiments showed that it was not practical to use our established mode of operation for subcritical walls because the entire flow field downstream of the model quarter chord became supersonic, and we were not able to establish flow field control. Subsequent experiments showed that a practical operational mode is to use wall control first to establish the desired distributions of the longitudinal velocity component for conditions where the walls are subcritical, and then to increase the Mach number and to readjust the wall control sequentially. In this way, we were able to exert the desired control for conditions where the local Mach number on the airfoil was about 1.30 and the local Mach number at the control surfaces was 1.05.

Iteration experiments with the 6%-blockage model were not attempted at this test condition, $M_\infty = 0.85$, $\alpha = 1^\circ$, because we were limited locally by the available wall control. A generalized analysis of the test section and auxiliary control circuit was performed to determine the relative tradeoffs between a larger compressor, increased wall porosity, model position, and model size. It was concluded that the most practical alternative, in this instance, was to build and test a 4%-blockage model.

A model with a solid blockage of 4% was built and exploratory experiments were performed at $M_\infty = 0.85$, $\alpha = 1^\circ$. These experiments consisted of using wall control to establish our first approximation for the model flow field and then to attempt iteration. Initial efforts were unsuccessful and subsequent experiments showed that the flow field corresponding to the first approximation was not steady. The shock waves on the airfoil fluctuated over about 15% of the model chord with a period of about ten seconds. Future experiments with supercritical walls will be based upon a test condition where these fluctuations are not observed.

ERRATA

AEDC-TR-78-36, November 1978
(UNCLASSIFIED REPORT)

RESEARCH ON ADAPTIVE WALL WIND TUNNELS

R. J. Vidal and J. D. Erickson, Jr.

Calspan Corporation
Buffalo, New York 14221

Page 26 was unintentionally omitted from subject report. This page is printed on the reverse side of this errata sheet. Please insert it in your copy of AEDC-TR-78-36.

REFERENCES

1. Sears, W.R. "Self-Correcting Wind Tunnels" (The Sixteenth Lanchester Memorial Lecture) The Aeronautical Journal, Vol. 78, No. 758/759, February/March 1974, pp. 80-89.

2. Ferri, A. and Baronti, P. "A Method for Transonic Wind Tunnel Corrections" AIAA Journal, Vol. 11, No. 1, January 1973, pp. 63-66.

3. Erickson, J.C., Jr., and Nenni, J.P. "A Numerical Demonstration of the Establishment of Unconfined-Flow Conditions in a Self-Correcting Wind Tunnel" Calspan Report No. RK-5070-A-1, November 1973.

4. Vidal, R.J., Catlin, P.A. and Chudyk, D.W. "Two-Dimensional Subsonic Experiments with an NACA 0012 Airfoil" Calspan Report No. RK-5070-A-3, December 1973.

5. Vidal, R.J., Erickson, J.C., Jr., and Catlin, P.A. "Experiments With a Self-Correcting Wind Tunnel" AGARD CP No. 174 on Wind Tunnel Design and Testing Techniques, October 1975.

6. Sears, W.R., Vidal, R.J., Erickson, J.C., Jr., and Ritter, A. "Interference-Free Wind-Tunnel Flows by Adpative-Wall Technology" Journal of Aircraft, Vol. 14, No. 11, November 1977, pp. 1042-1050.

7. Chew, W.L. "Cross-Flow Calibration at Transonic Speeds of Fourteen Perforated Plates With Round Holes and Airflow Parallel to the Plates" AEDC-TR-54-65, July 1955.

8. Murman, E.M., Bailey, F.R. and Johnson, M.L. "TSFOIL- A Computer Code for Two-Dimensional Transonic Calculations, Including Wind-Tunnel Wall Effects and Wave-Drag Evaluation" Paper No. 26 in Aerodynamic Analyses Requiring Advanced Computers, NASA-SP-347-Part 2, March 1975.

APPENDIX

There were three experimental and theoretical efforts carried out in direct support of the experiments. The first of these is the extended calibration of the flow angle probes. The second is the estimation of the disturbance velocity components at the control surface locations in order to start the experimental iterations. The third is the evaluation of the exterior-flow functional relationships during the experimental iterations toward unconfined flow.

A.1 PROBE CALIBRATION

One task that was completed early in the research was the calibration of probes for measuring the flow angle over a more complete range of Mach number. A typical probe is shown schematically in Fig. 2, and the flow angle sensor consists of two hypodermic tubes mounted side by side with the front faces chamfered at $\pm 45^{\circ}$. The static pressure orifices shown in Fig. 2 are not used because of excessive interference from the probe stem. The probes were mounted in a fixture located behind the tunnel wall at a longitudinal position about 10 inches upstream of mid-tunnel. This fixture positioned the probes at flow angles of ± 4 degrees. Since the exposed length of the probe stems was identical to that used in the experiments with the airfoil in place, there was no need to consider probe deflections. Active wall control was used to establish a uniform static pressure distribution along the length of the test section in order to approximate parallel flow. Calibrations were obtained at discrete Mach numbers up to 0.95, and all test conditions were repeated several times to determine the scatter in the data. Following these experiments, the probes were remounted through the walls at the longitudinal positions used in the airfoil experiments. The tunnel then was run without the model, wall control was used to obtain a uniform longitudinal pressure distribution in the test section, and the probe readings were taken to be those corresponding to parallel flow. Again, the experiments were repeated several times to determine the scatter.

These experiments determined the slopes of the calibration curves as a function of Mach number. It was found that the slopes increased or decreased, depending on the individual probe, and there were no abrupt changes in the slopes or probe zeros within the Mach number range tested. Nominally, the incompressible probe sensitivity is $\frac{\Delta p}{q} \approx 2 \sin \alpha$, and the Mach number effects change this value by about 10% at $M_\infty = 0.95$.

A.2 ESTIMATES OF THE DISTURBANCE VELOCITY COMPONENTS

In the experiments to establish an operational mode, estimates of the disturbance velocity components at the control surfaces were made on the basis of Prandtl-Glauert theory. It was assumed that the airfoil model can be represented by a source, vortex and streamwise doublet, the strengths of which are proportional to the airfoil drag, lift and thickness, respectively. Although these initial estimates are adequate at subcritical Mach numbers, they are less satisfactory at $M_\infty = 0.85$ and 0.90. After the operational mode experiments, therefore, the NASA/Ames computer program TSFOIL[8] was made operational on the IBM 360/65 computer at Calspan. Thus, both a Prandtl-Glauert method and TSFOIL are now available to provide estimates of the flow field.

A.3 EVALUATION OF THE FUNCTIONAL RELATIONSHIPS

An effort was devoted to improving our functional-relationship evaluation techniques. That is, in preparation for the experiments with supercritical flow at the control surfaces, we modified the transonic finite-difference computer program for evaluating the unconfined flow functional relationships. This program was developed at Calspan by Dr. W. J. Rae and was modified by him later to treat control surface measurements at two different distances from the model, as in our experimental arrangement. The modifications have been along the lines of streamlining the handling procedure of typical input data and of providing the appropriate printout and computer plots of the results. Two programs were made operational. The first of these carries out a cubic spline fit to the measured normal velocity data and then evaluates the corresponding unconfined-flow values of the longitudinal

8. Murman, E.M., Bailey, F.R. and Johnson, M.L. "TSFOIL-A Computer Code for Two-Dimensional Transonic Calculations, Including Wind-Tunnel Wall Effects and Wave-Drag Evaluation" Paper No. 26 in Aerodynamic Analyses Requiring Advanced Computers, NASA-SP-347-Part 2, March 1975.

velocity. The second program carries out a smoothing spline fit to the measured longitudinal velocity data and evaluates the corresponding unconfined flow values of the normal velocity.

As indicated in Section 2, we concluded that we must continue to set the longitudinal velocity component u in the experiments. This requires that the distributions of the measured normal velocity component v_m be used as the boundary conditions on the external-flow calculations to provide the next approximation to u . We had found earlier in our experiments, however, that it is difficult to carry out conventional interpolation procedures accurately based on the small number of v_m measurements available (ten at the upper control surface, eight at the lower). Fortunately, however, we do have a sufficient number of u_m measurements (forty to fifty at each control surface) to provide a good definition of their distributions. Based on the existing situation, we have devised a procedure which should provide an adequate interpolation in the v_m data, especially if we are not too far from unconfined-flow conditions.

The first step in this interpolation procedure is to use the extensive u_m data, as interpolated by a cubic spline (smoothed or not, as desired), to calculate the corresponding unconfined flow distribution $v_c\,[u_m]$. Next, the difference $v_m - v_c\,[u_m]$ is determined at each x_m location where v_m measurements are made. These differences are then interpolated linearly in x, so that the resultant interpolation in v_m is found by adding the interpolated difference, $v_m - v_c\,[u_m]$, to the calculated $v_c\,[u_m]$ distribution. Once the v_m interpolation has been found, the exterior-flow calculation of $u_c\,[v_m]$ is carried out to give the next approximation to u which will be set in the tunnel.

This procedure thus uses the shape of the $v_c\,[u_m]$ distribution as a basis for interpolation since the u_m distribution is well defined experimentally. Clearly, as convergence of the tunnel iteration is approached, the differences $v_m - v_c\,[u_m]$ will approach zero and the interpolation should improve. To date, this method has not been exercised in iteration experiments.

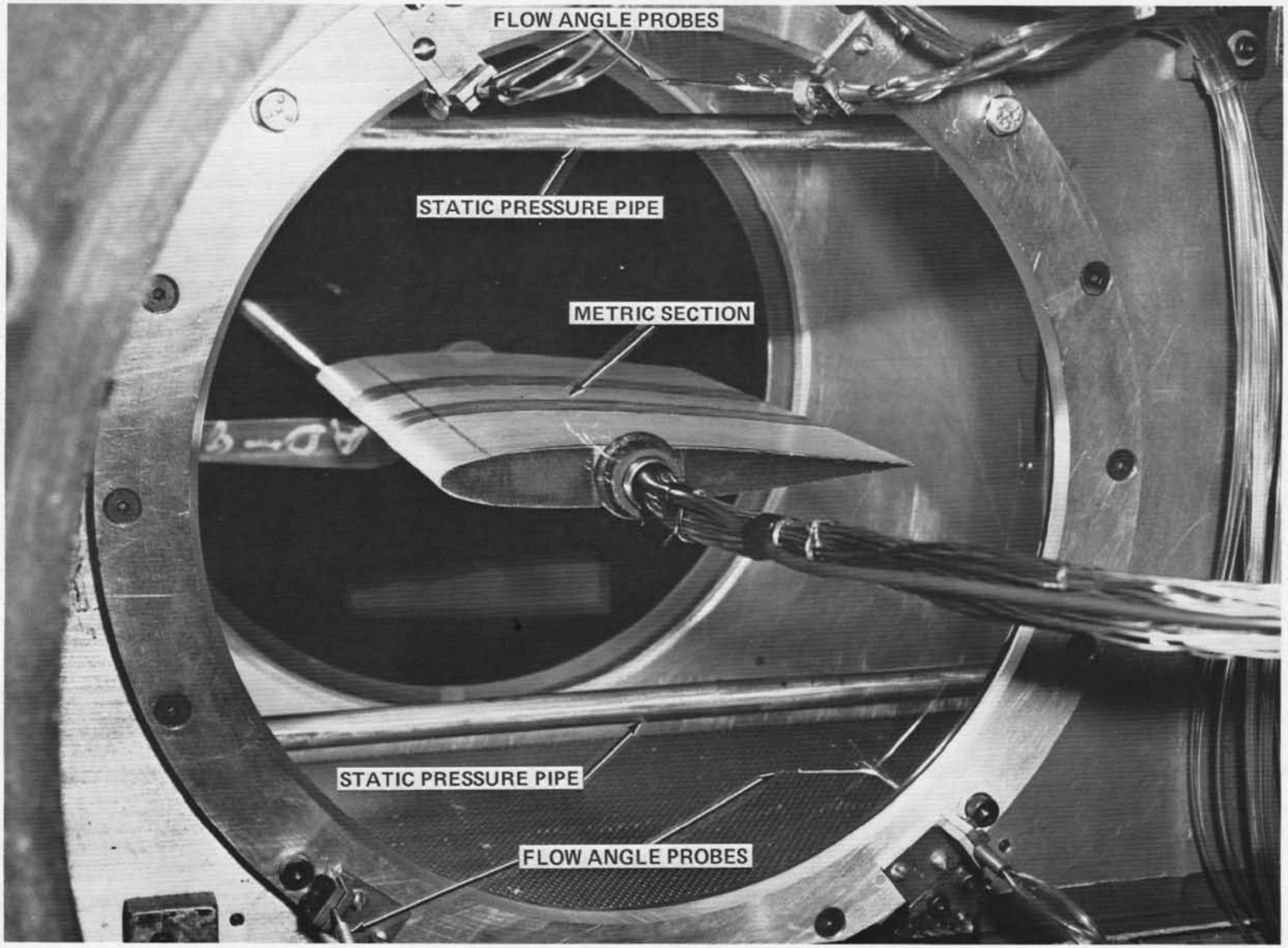

Figure 1 TEST SECTION OF THE SELF-CORRECTING WIND TUNNEL WITH THE 6% BLOCKAGE MODEL

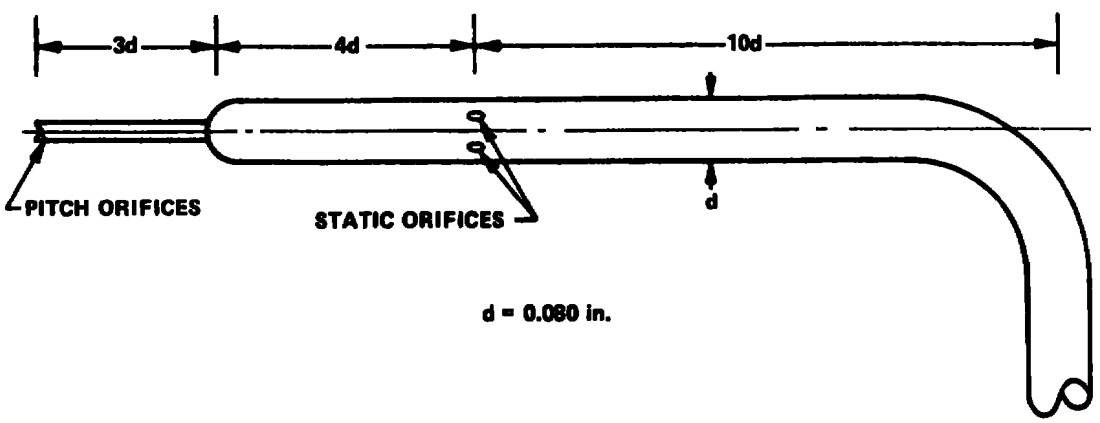

Figure 2 PITCH-STATIC PRESSURE SENSOR

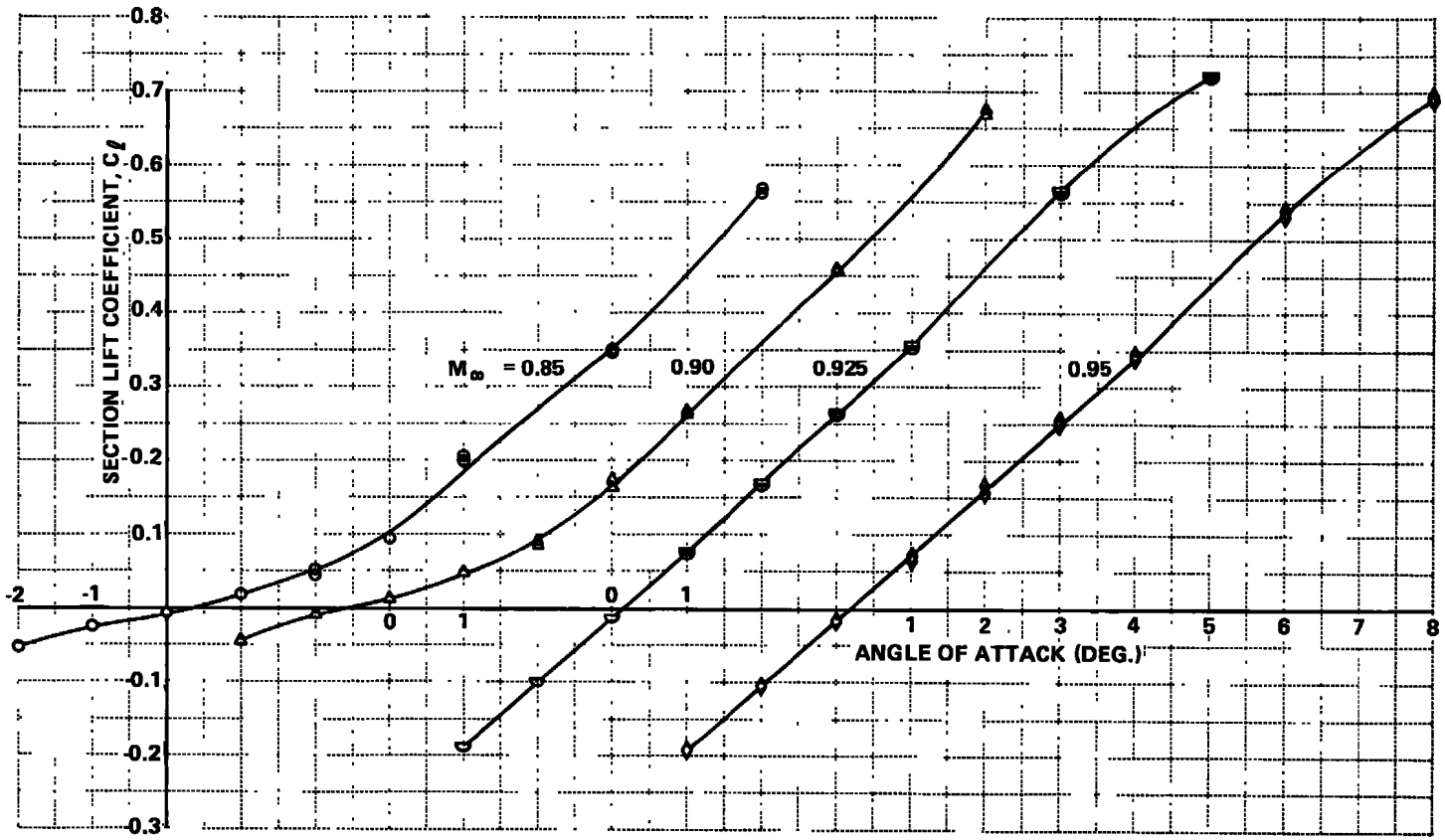

Figure 3 SECTION LIFT COEFFICIENT FOR A 6-INCH CHORD, NACA 0012 AIRFOIL, Re = 10^6 , 8-FT TUNNEL DATA

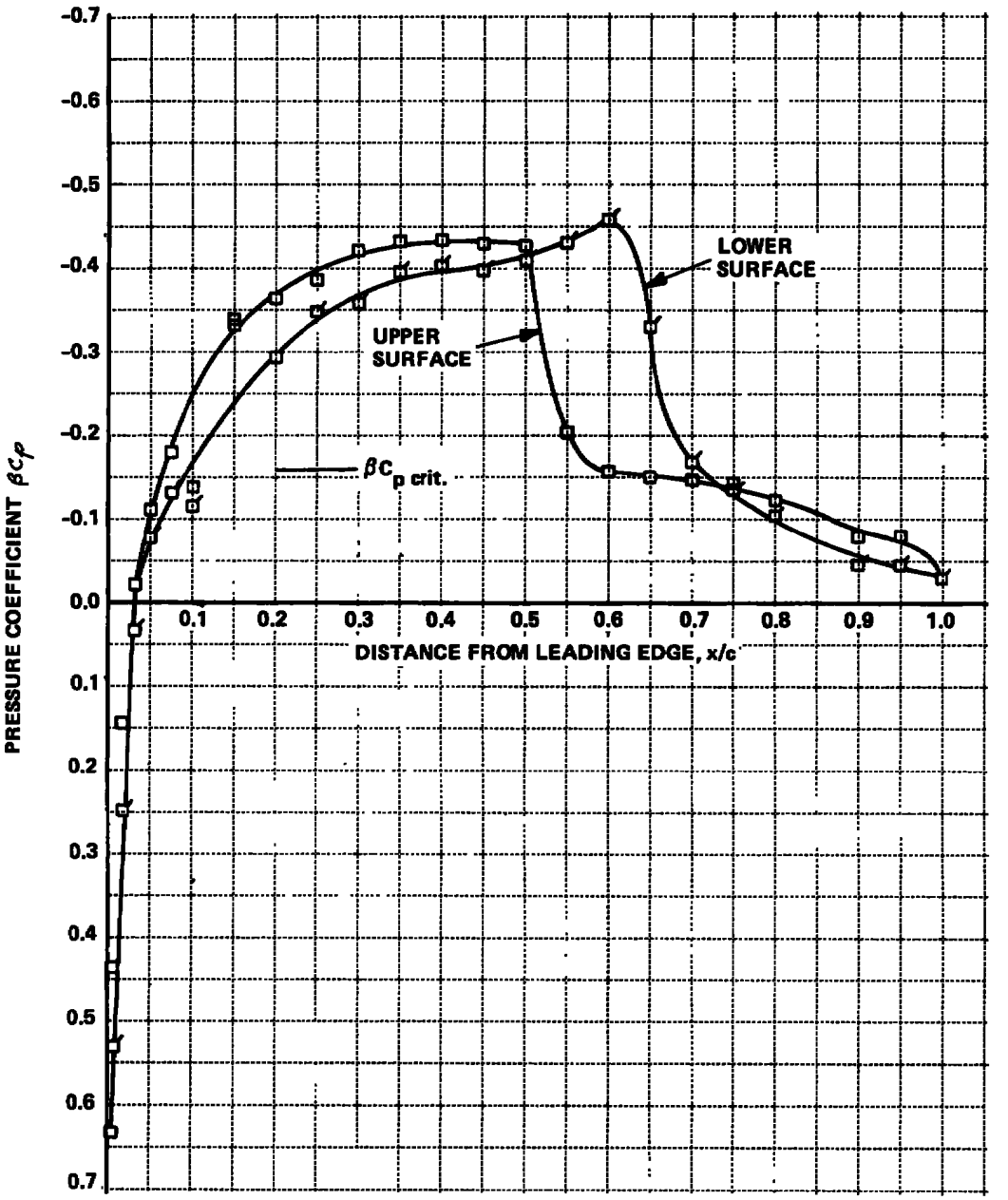

Figure 4 PRESSURE DISTRIBUTIONS ON THE 6-INCH CHORD, 0012 AIRFOIL $M_\infty = 0.85$, $\alpha = 1^o$ 8-FT TUNNEL DATA

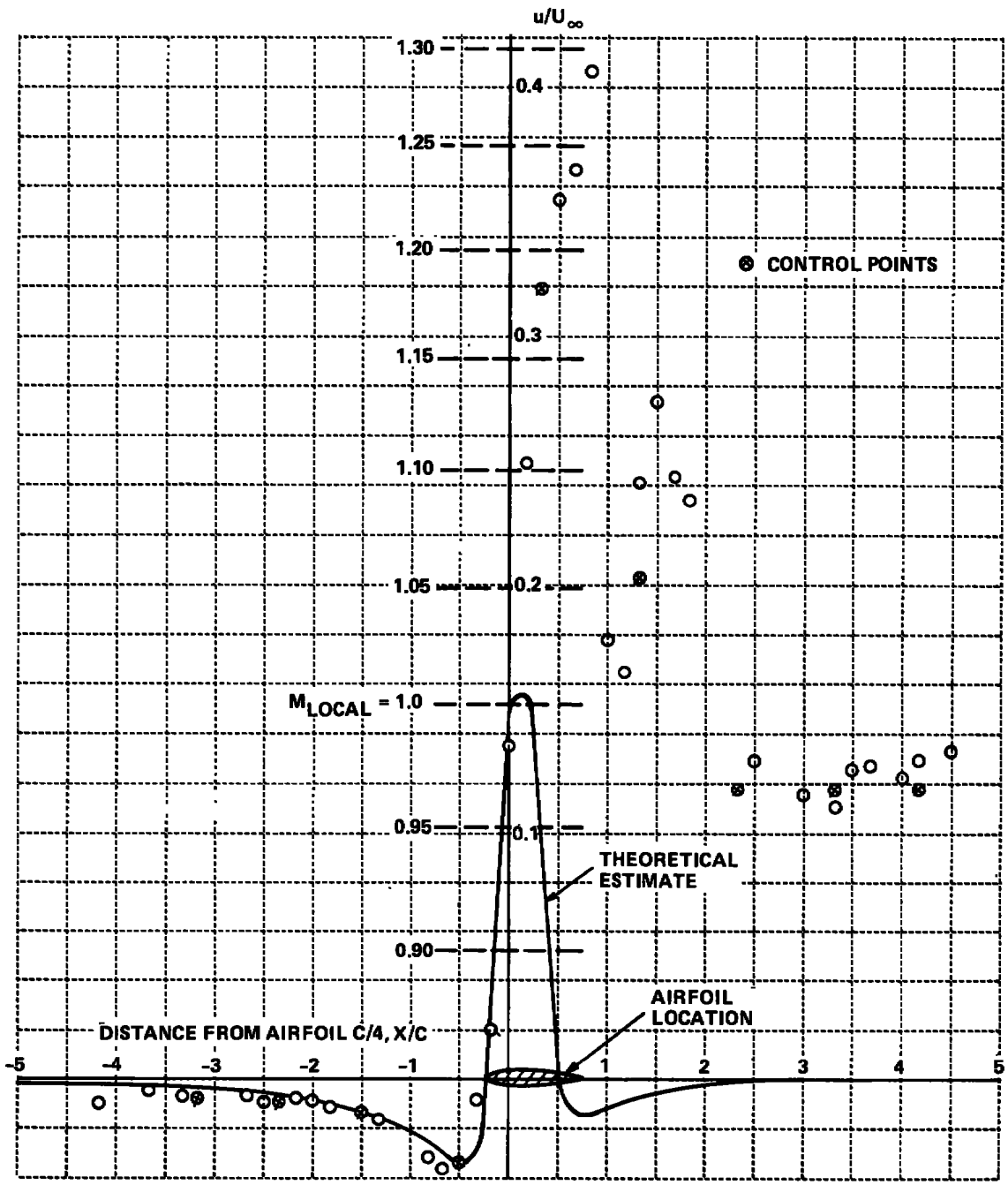

Figure 5 LONGITUDINAL DISTURBANCE VELOCITY AT THE UPPER CONTROL SURFACE USING SUBCRITICAL CONTROL PROCEDURE, 6% BLOCKAGE.
$h/c = +0.653$, $M_\infty = 0.85$, $\alpha = 1^\circ$

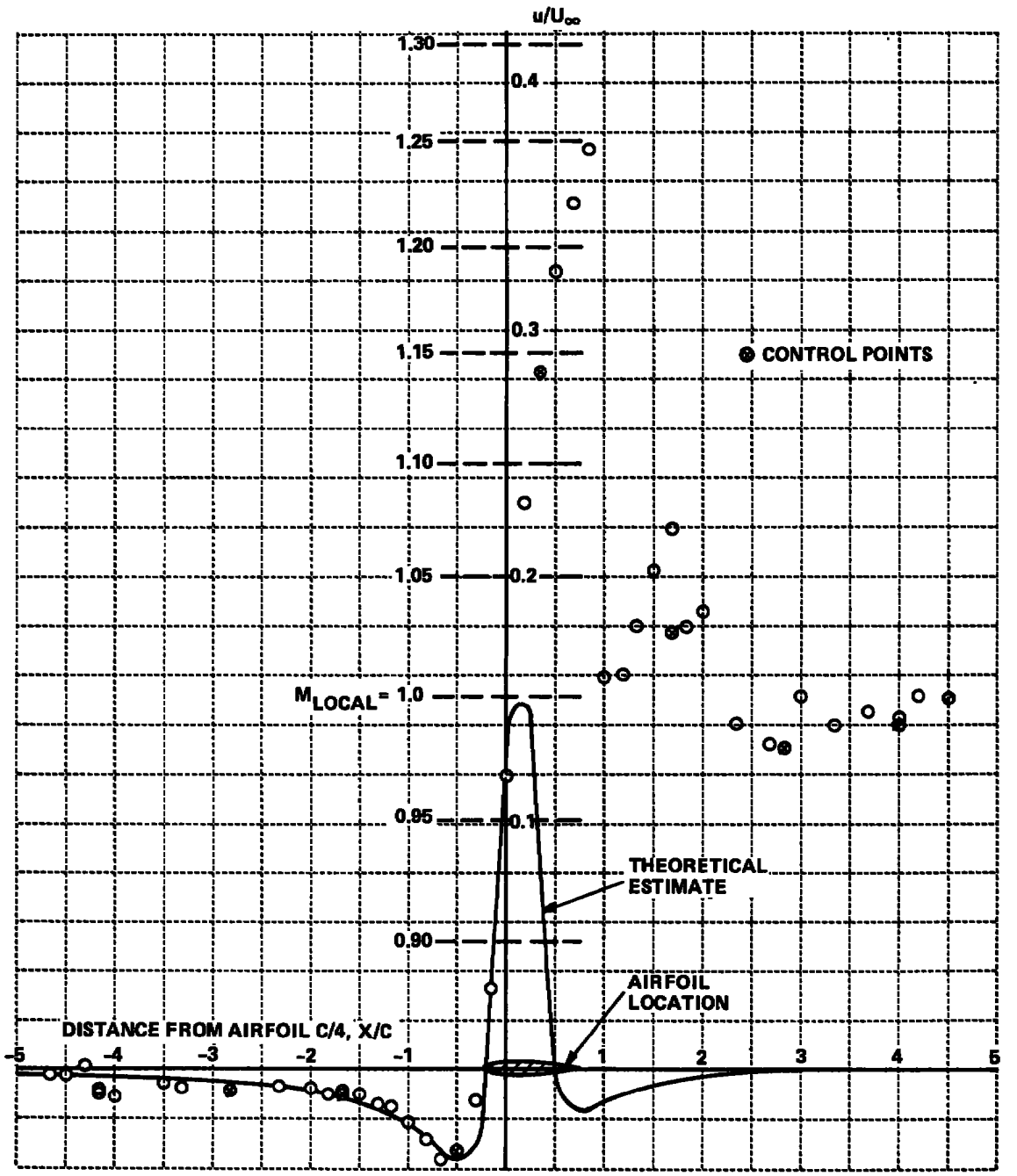

Figure 6 LONGITUDINAL DISTURBANCE VELOCITY AT THE LOWER CONTROL SURFACE USING SUBCRITICAL CONTROL PROCEDURE, 6% BLOCKAGE. $h/c = -0.657$, $M_\infty = 0.85$, $\alpha = 1^0$

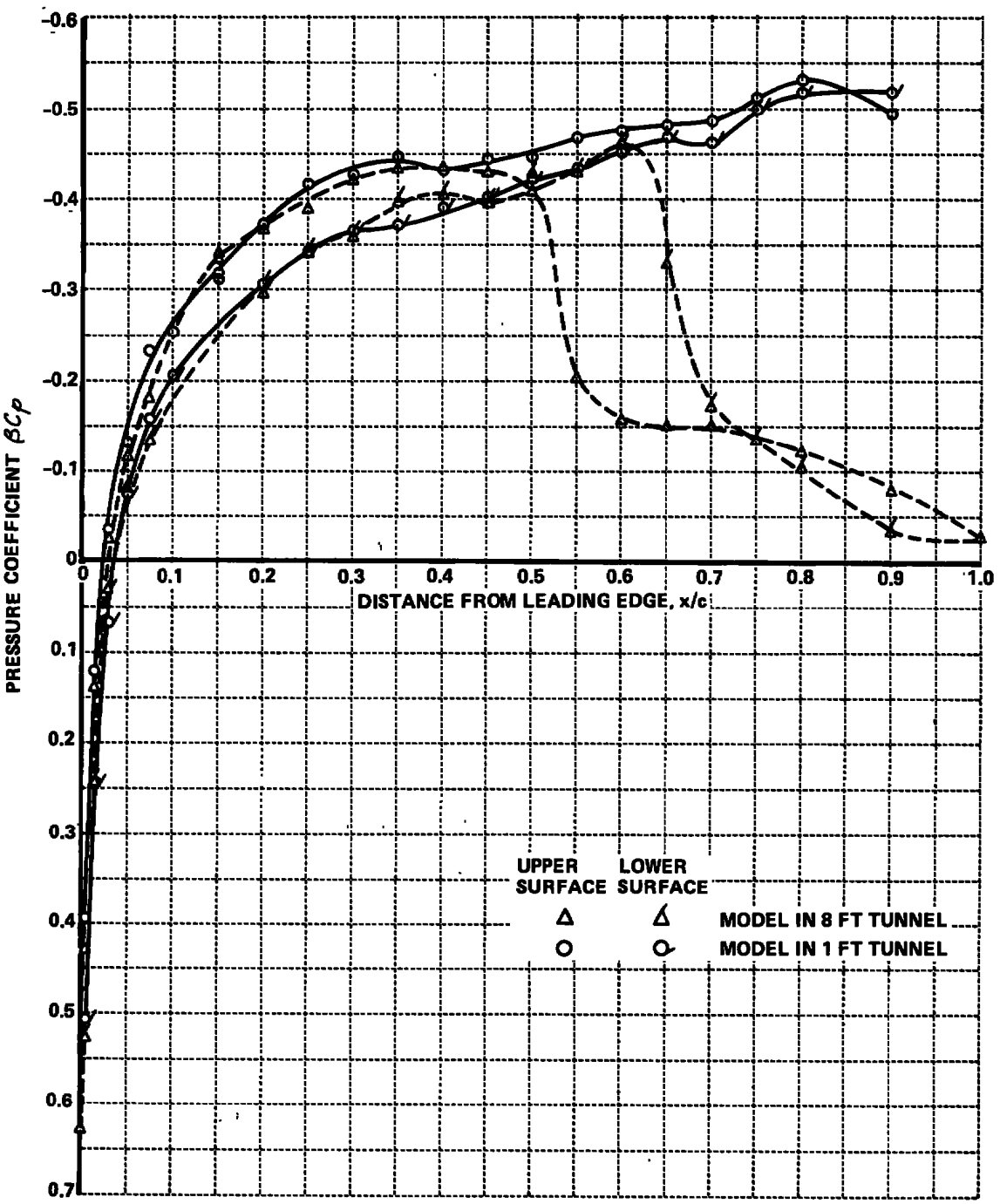

Figure 7 COMPARISON OF AIRFOIL PRESSURE DISTRIBUTIONS, SUBCRITICAL CONTROL PROCEDURE, 6% BLOCKAGE. $M_\infty = 0.85$, $\alpha = 1^o$

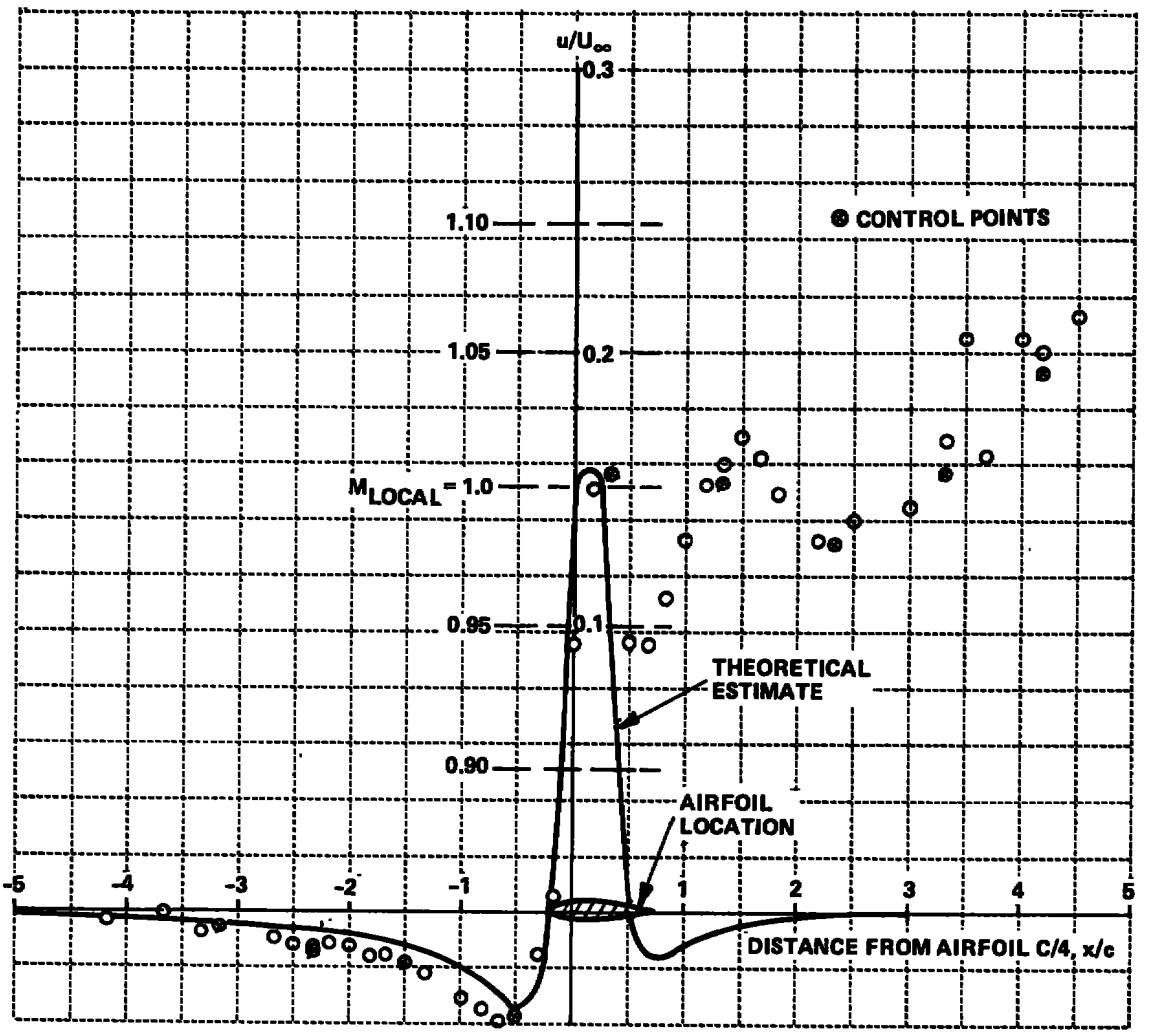

Figure 8 LONGITUDINAL DISTURBANCE VELOCITY AT THE UPPER CONTROL SURFACE USING MODIFIED CONTROL PROCEDURE, 6% BLOCKAGE.
$h/c = +0.653$, $M_\infty = 0.85$, $\alpha = 1^\circ$

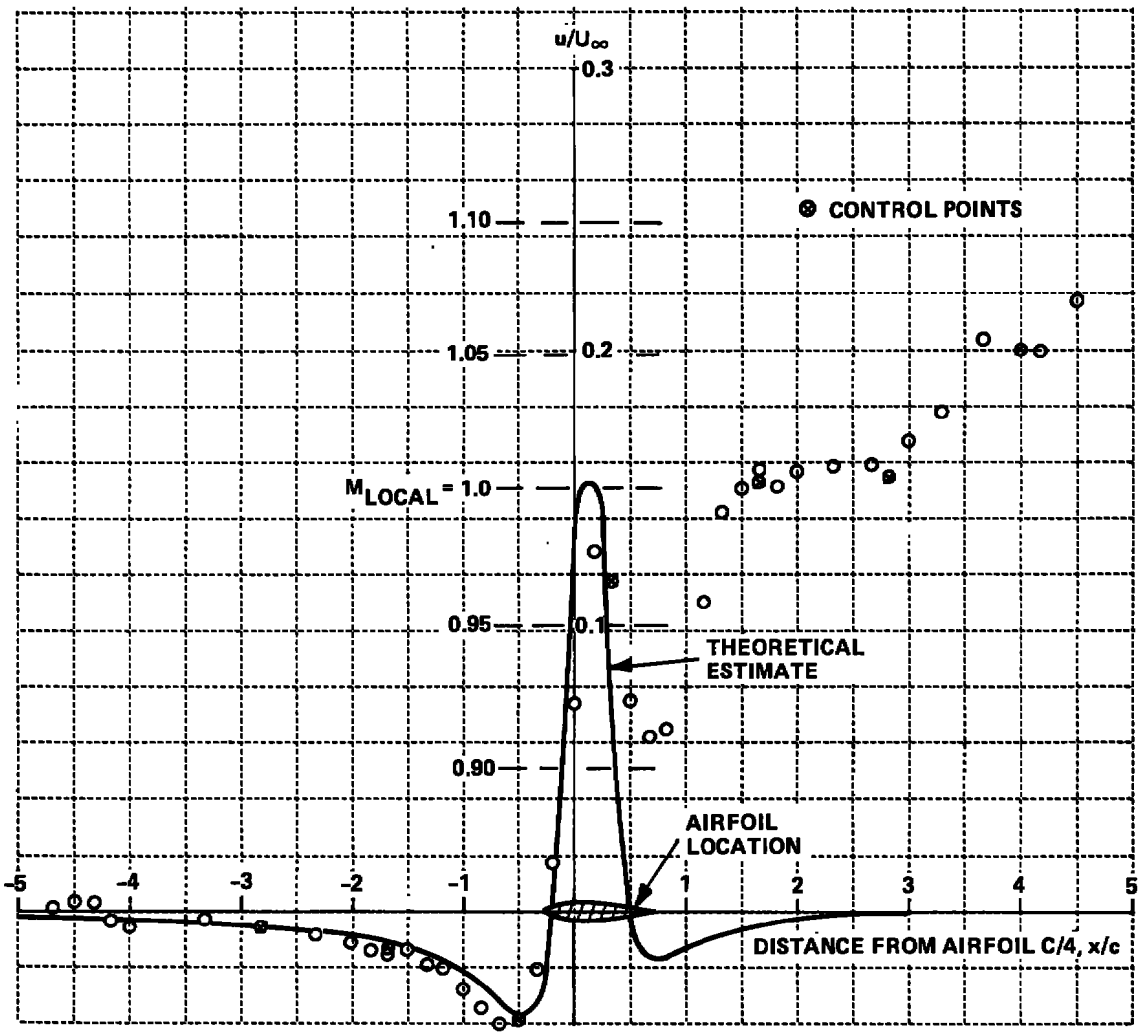

Figure 9 LONGITUDINAL DISTURBANCE VELOCITY AT THE LOWER CONTROL SURFACE USING MODIFIED CONTROL PROCEDURE, 6% BLOCKAGE. $h/c = -0.657$, $M_\infty = 0.85$, $\alpha = 1^0$

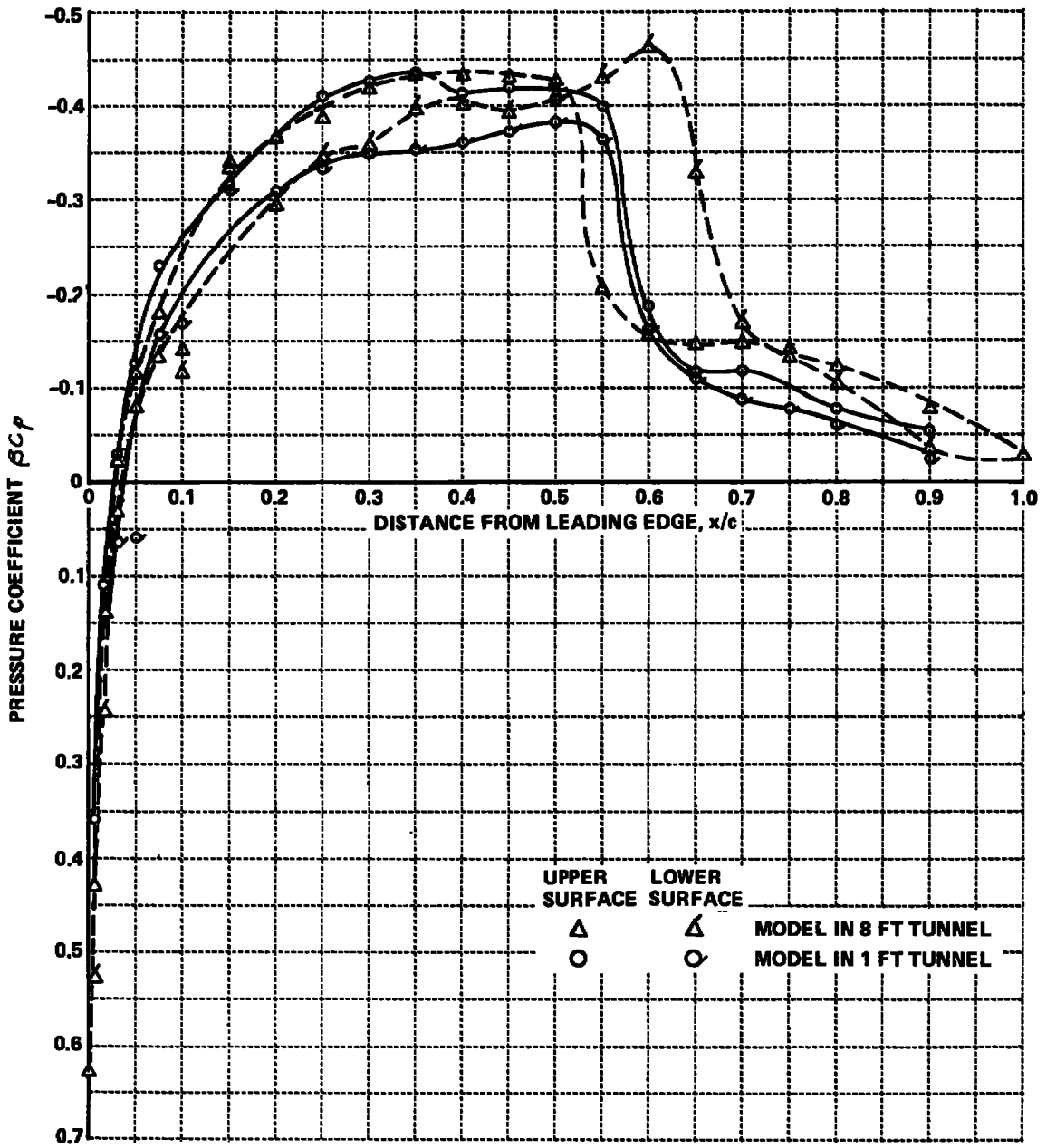

Figure 10 COMPARISON OF AIRFOIL PRESSURE DISTRIBUTIONS, MODIFIED CONTROL PROCEDURE, 6% BLOCKAGE. $M_\infty = 0.85$, $\alpha = 1^0$

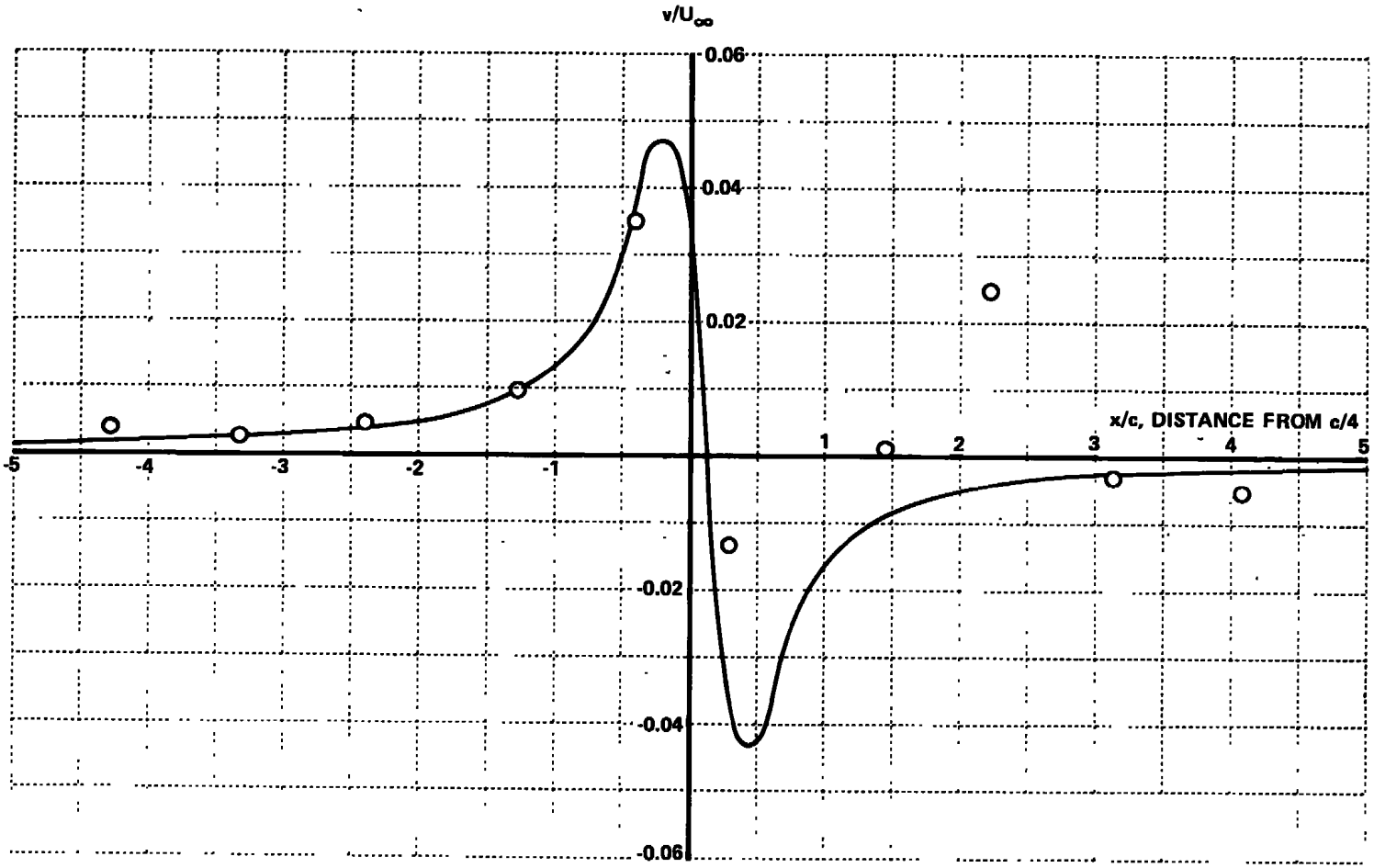

Figure 11 NORMAL VELOCITY COMPONENTS AT THE UPPER CONTROL SURFACE, $M_\infty = 0.80$, $\alpha = 1^o$, 6% BLOCKAGE. WALL CONTROL USED TO ESTABLISH NORMAL VELOCITY COMPONENTS

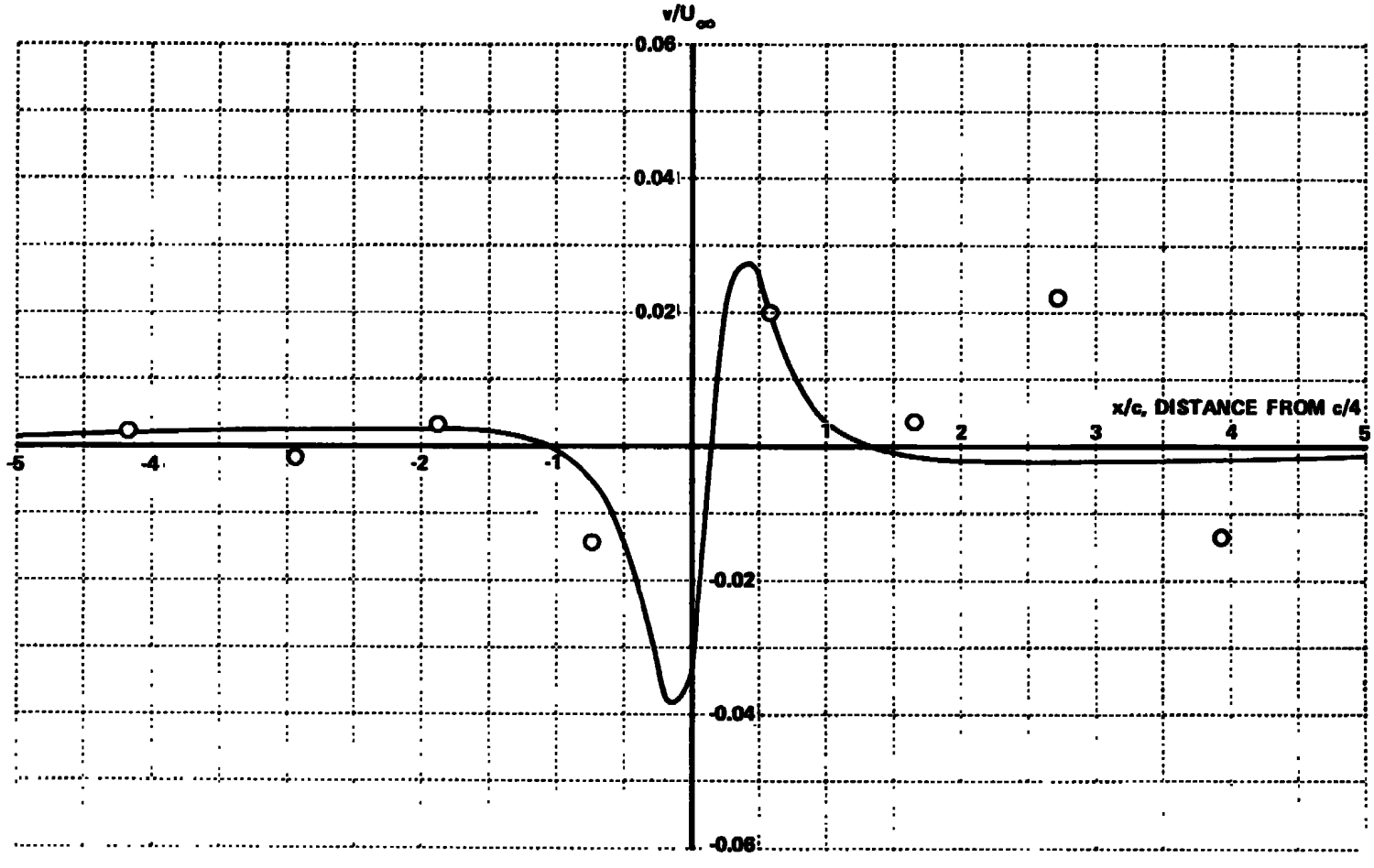

Figure 12 NORMAL VELOCITY COMPONENTS AT THE LOWER CONTROL SURFACE, $M_\infty = 0.80$, $\alpha = 1^0$, 6% BLOCKAGE. WALL CONTROL USED TO ESTABLISH NORMAL VELOCITY COMPONENTS

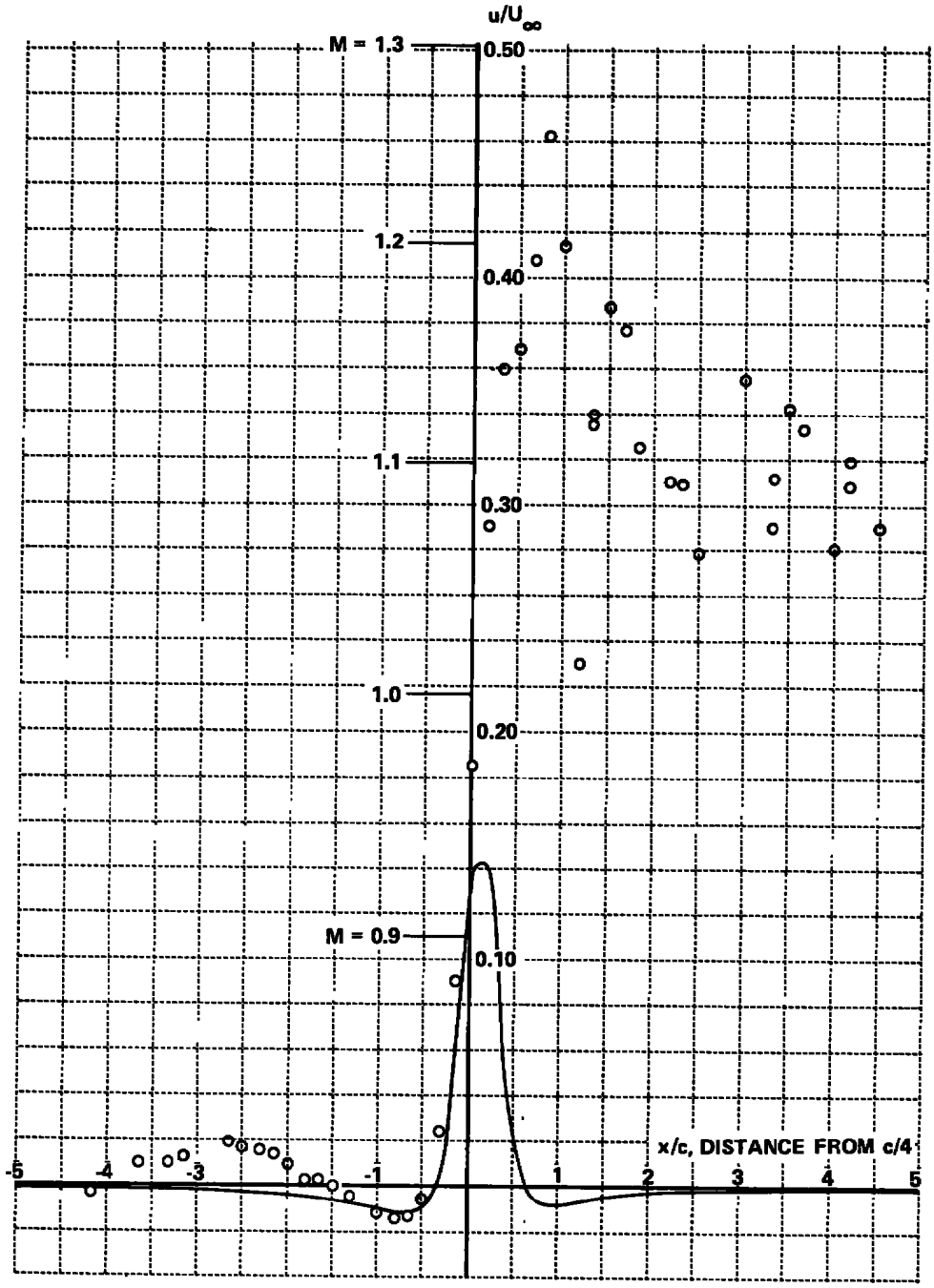

Figure 13 LONGITUDINAL VELOCITY COMPONENTS AT THE UPPER CONTROL SURFACE, $M_\infty = 0.80$, $\alpha = 1^o$, 6% BLOCKAGE. WALL CONTROL USED TO ESTABLISH NORMAL VELOCITY COMPONENTS

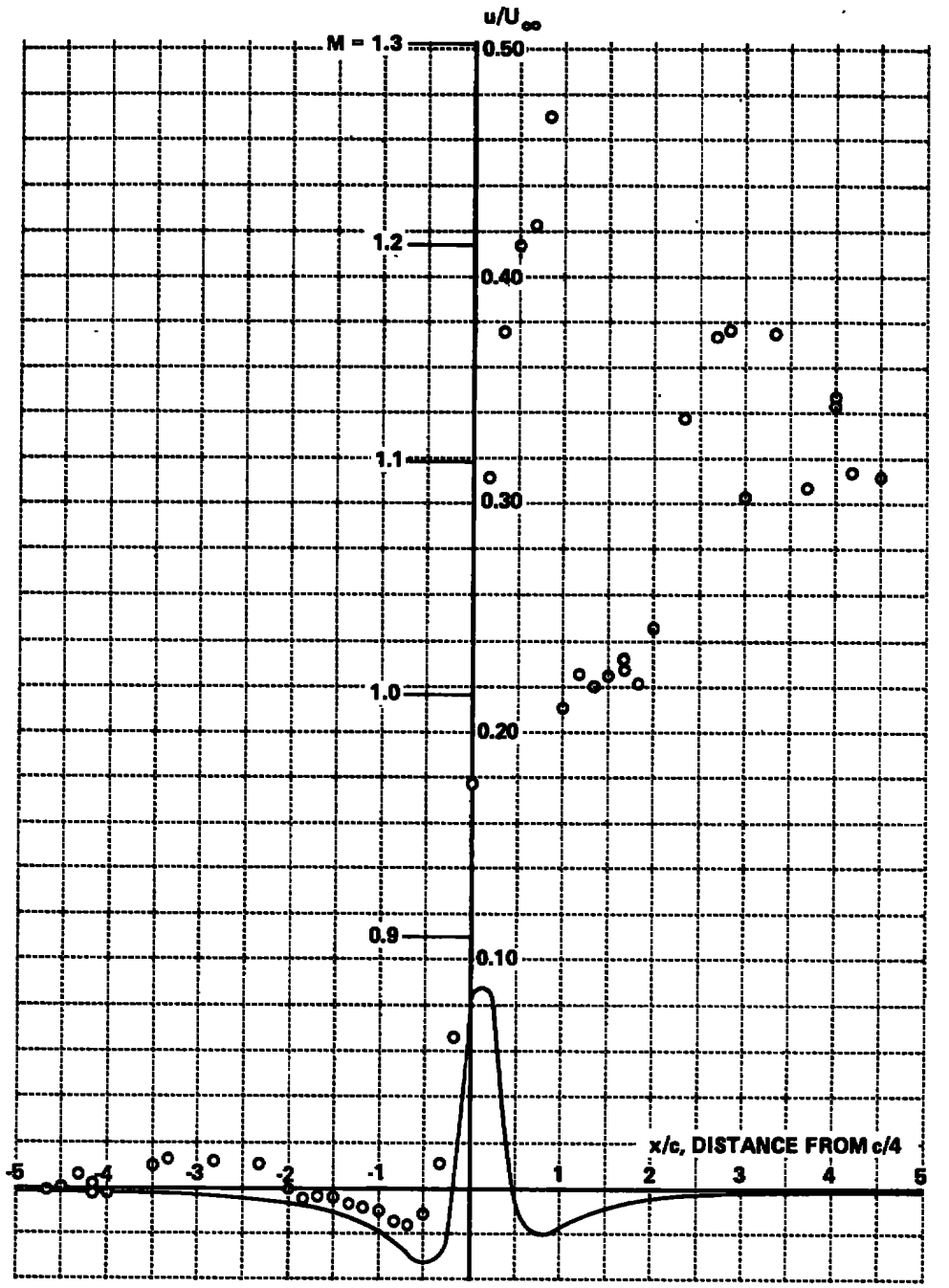

Figure 14 LONGITUDINAL VELOCITY COMPONENTS AT THE LOWER CONTROL SURFACE, $M_\infty = 0.80$, $\alpha = 1^o$, 6% BLOCKAGE. WALL CONTROL USED TO ESTABLISH NORMAL VELOCITY COMPONENTS.

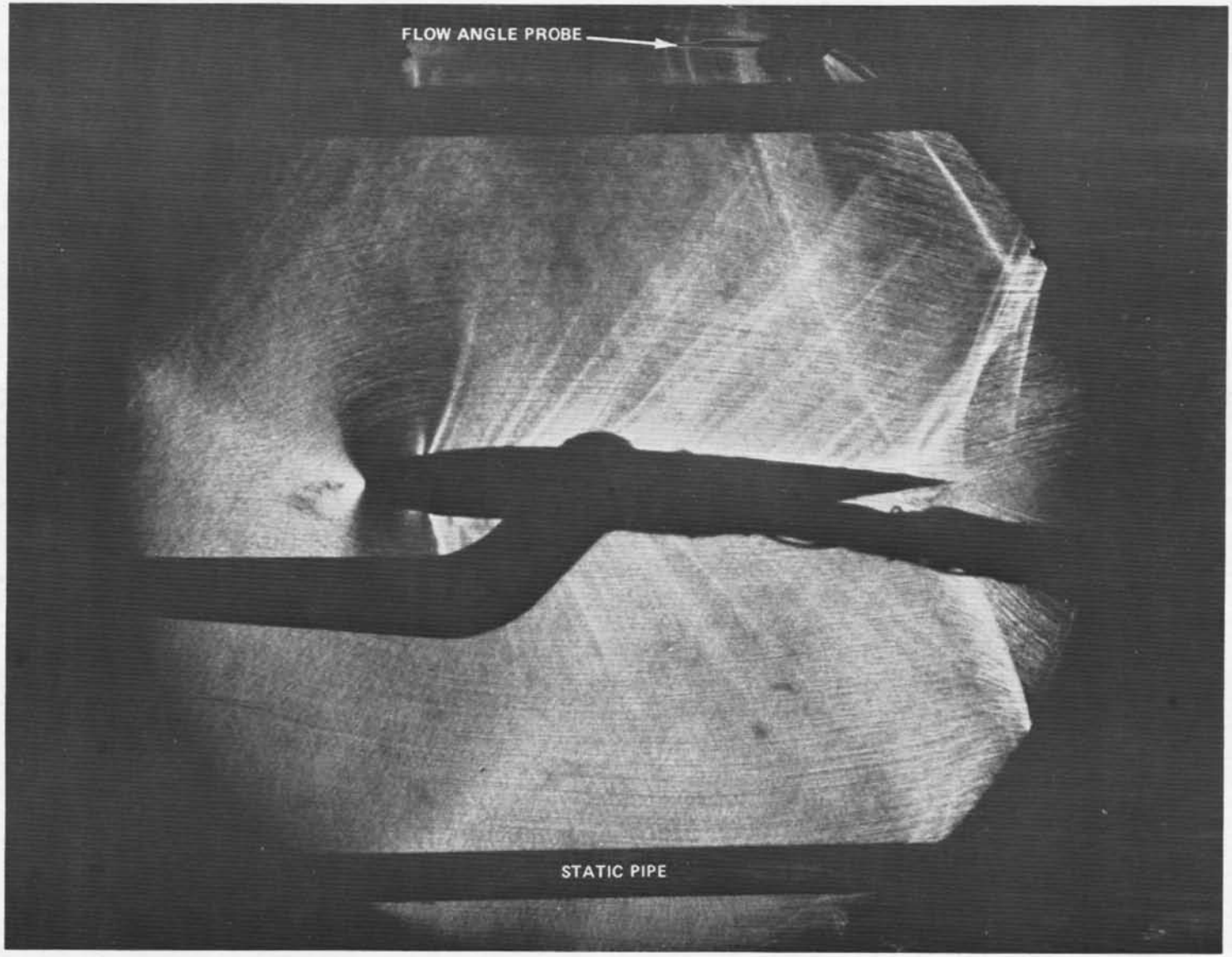

Figure 15 SCHLIEREN VIEW OF THE FLOWFIELD AT M_∞ = 0.80, α = 1°, 6% BLOCKAGE. WALL CONTROL USED TO ESTABLISH THE NORMAL VELOCITY COMPONENTS

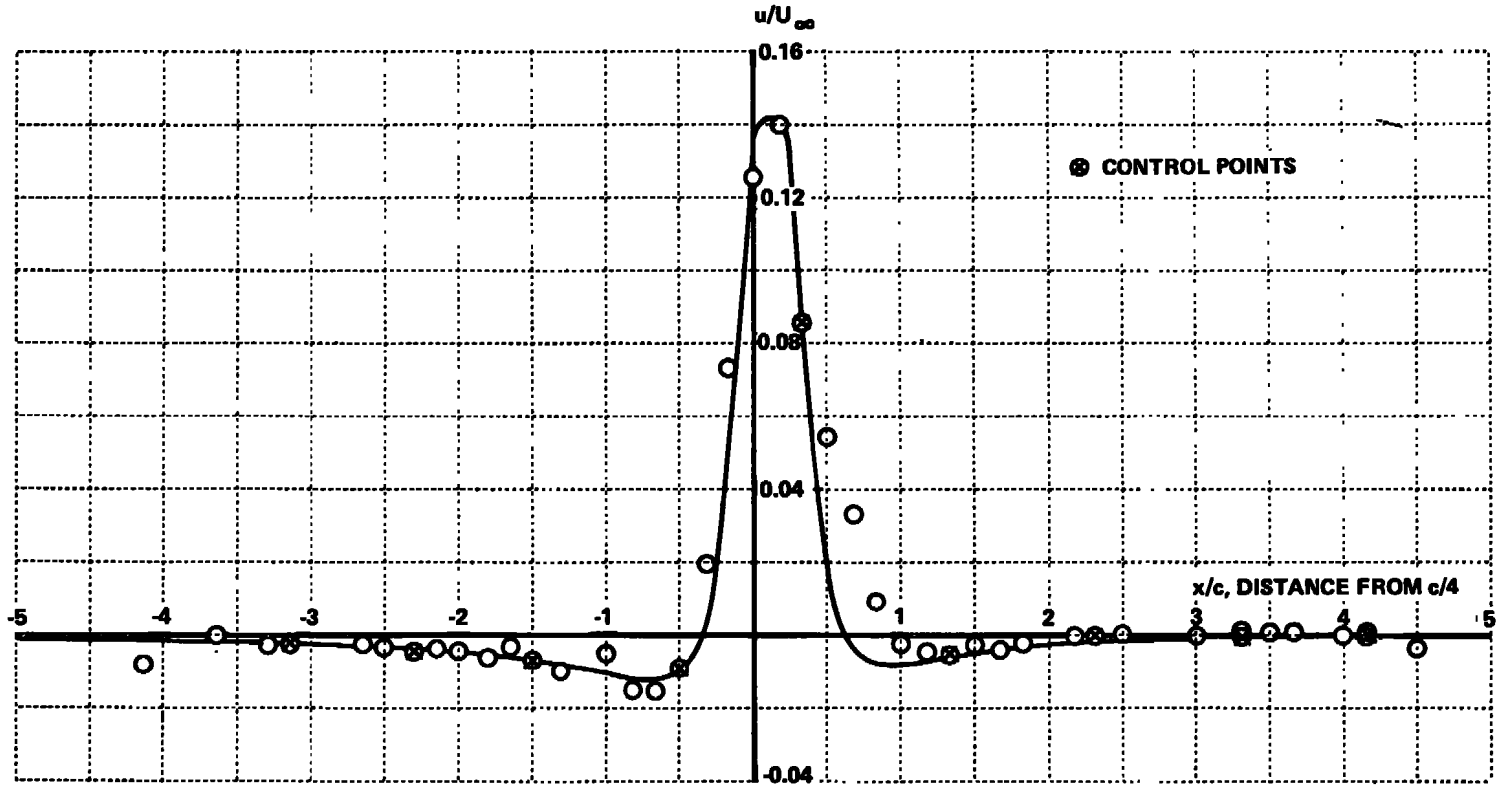

Figure 16 LONGITUDINAL VELOCITY COMPONENTS AT THE UPPER CONTROL SURFACE, $M_\infty = 0.80$, $\alpha = 1^o$, 6% BLOCKAGE. WALL CONTROL USED TO ESTABLISH LONGITUDINAL VELOCITY COMPONENTS

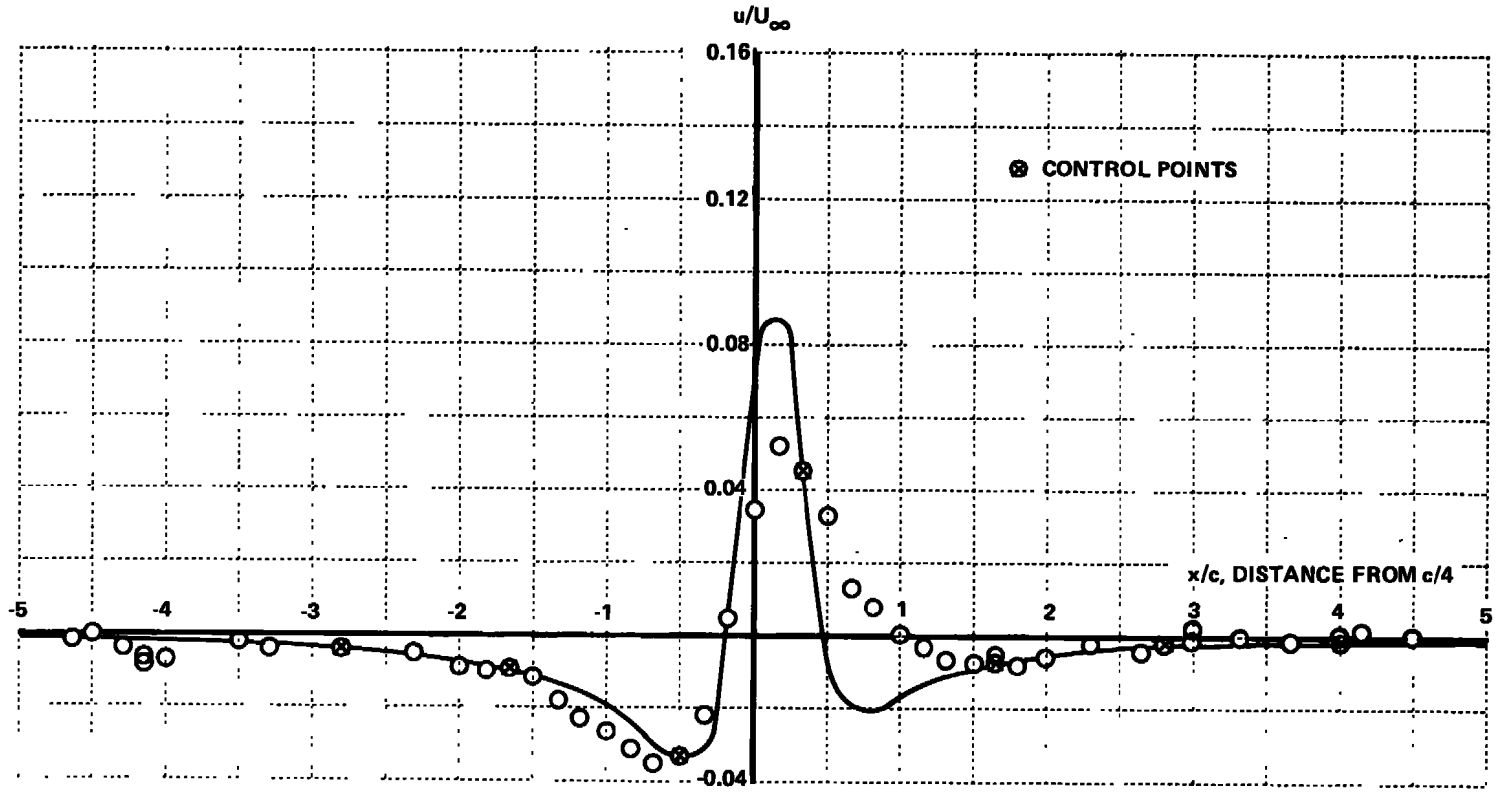

Figure 17 LONGITUDINAL VELOCITY COMPONENTS AT THE LOWER CONTROL SURFACE, $M_\infty = 0.80$, $\alpha = 1^o$, 6% BLOCKAGE. WALL CONTROL USED TO ESTABLISH LONGITUDINAL VELOCITY COMPONENTS

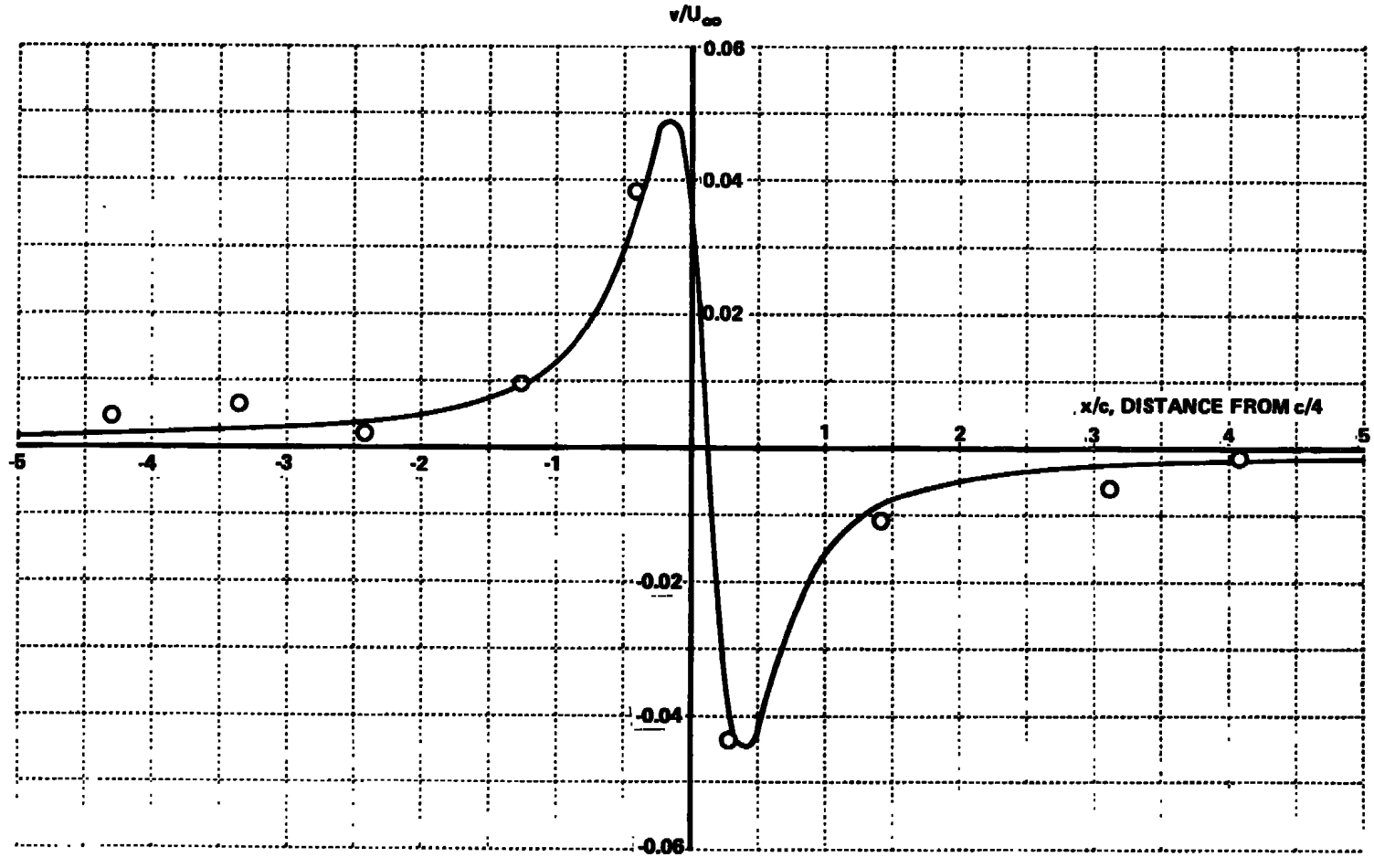

Figure 18 NORMAL VELOCITY COMPONENTS AT THE UPPER CONTROL SURFACE, $M_\infty = 0.80$, $\alpha = 1^\circ$, 6% BLOCKAGE. WALL CONTROL USED TO ESTABLISH LONGITUDINAL VELOCITY COMPONENTS

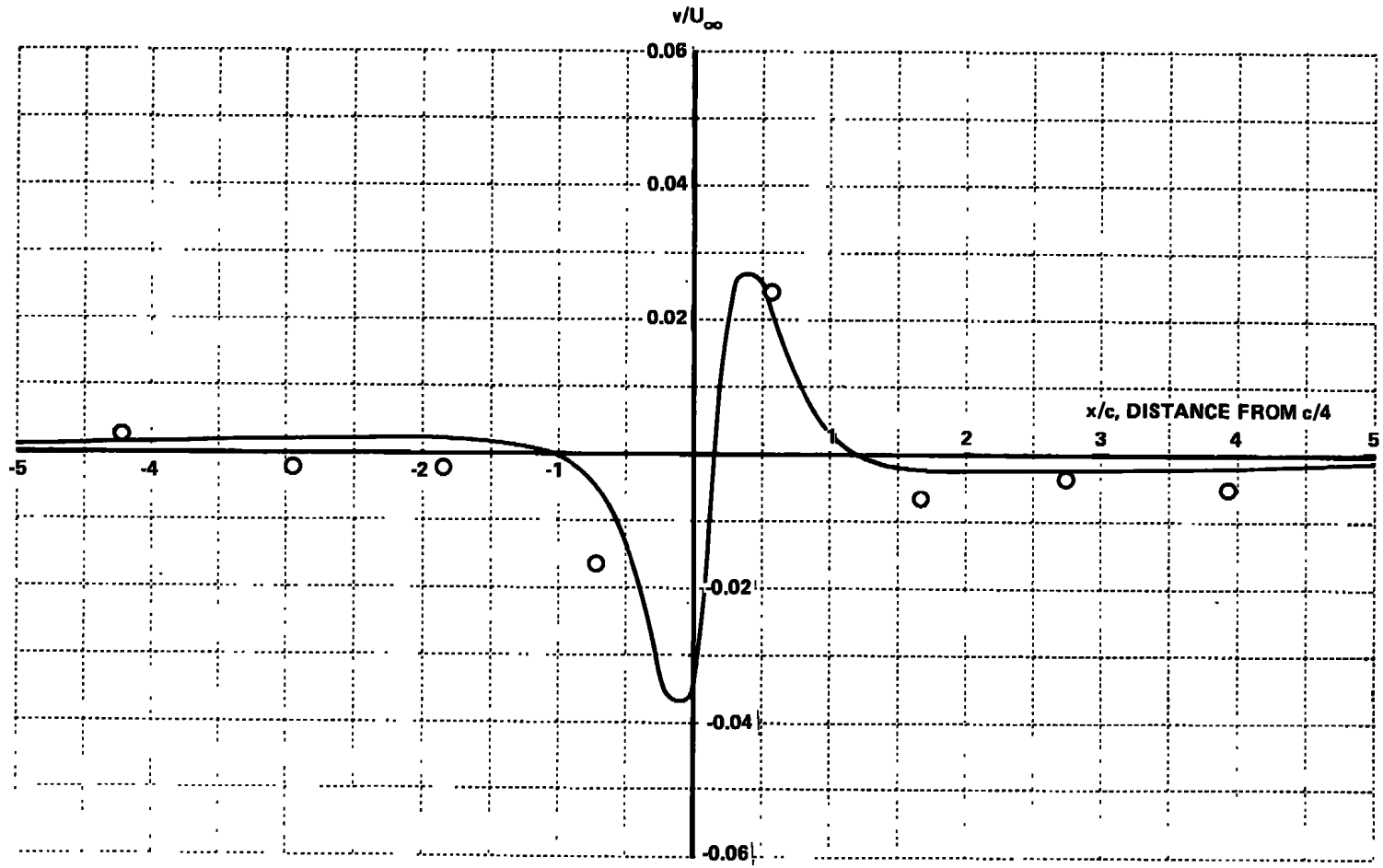

Figure 19 NORMAL VELOCITY COMPONENTS AT THE LOWER CONTROL SURFACE, M_∞= 0.80, α = 1°, 6% BLOCKAGE. WALL CONTROL USED TO ESTABLISH LONGITUDINAL VELOCITY COMPONENTS

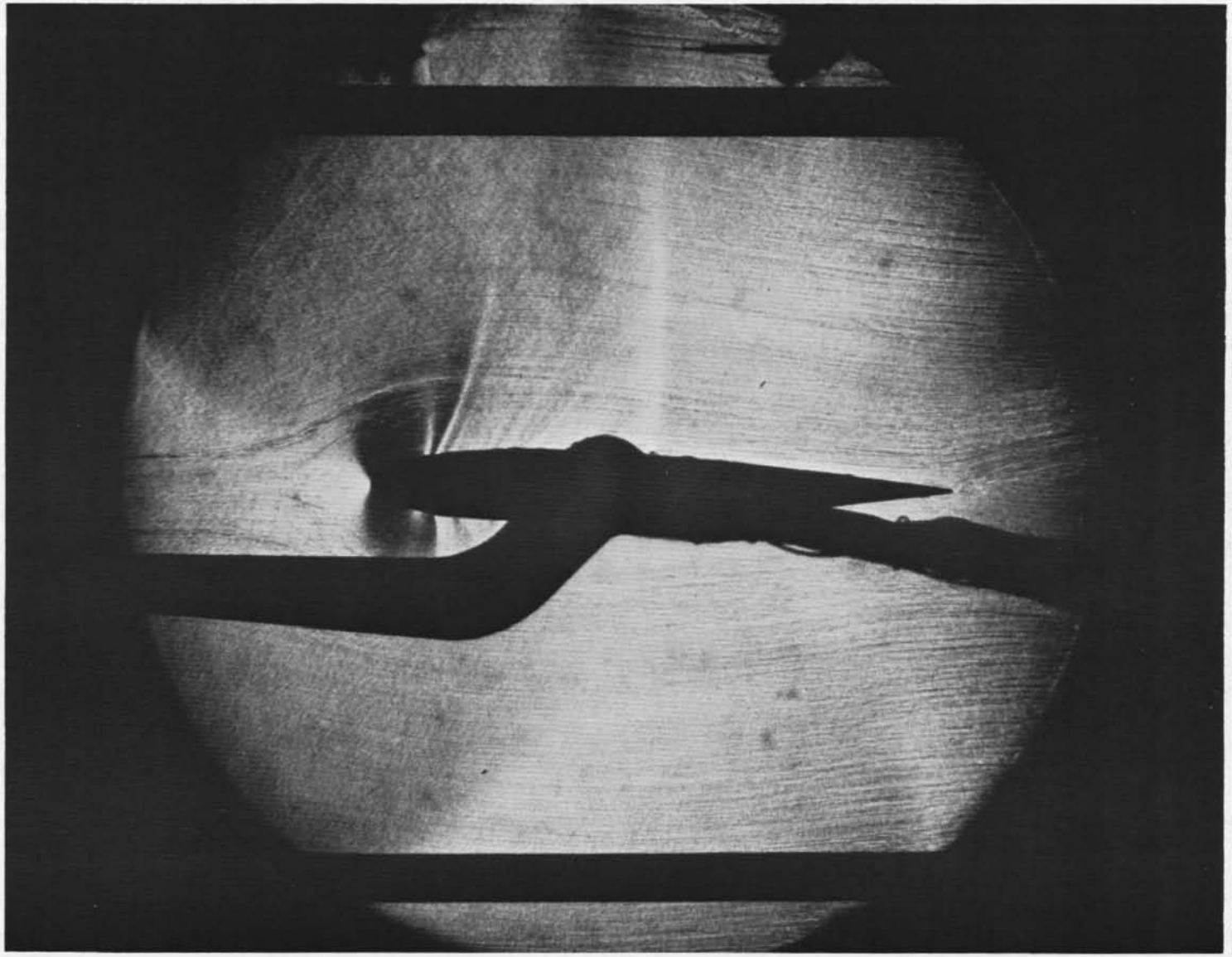

Figure 20 SCHLIEREN VIEW OF THE FLOW FIELD AT M_∞ = 0.80, α = 1°, 6% BLOCKAGE. WALL CONTROL USED TO ESTABLISH THE LONGITUDINAL VELOCITY COMPONENTS

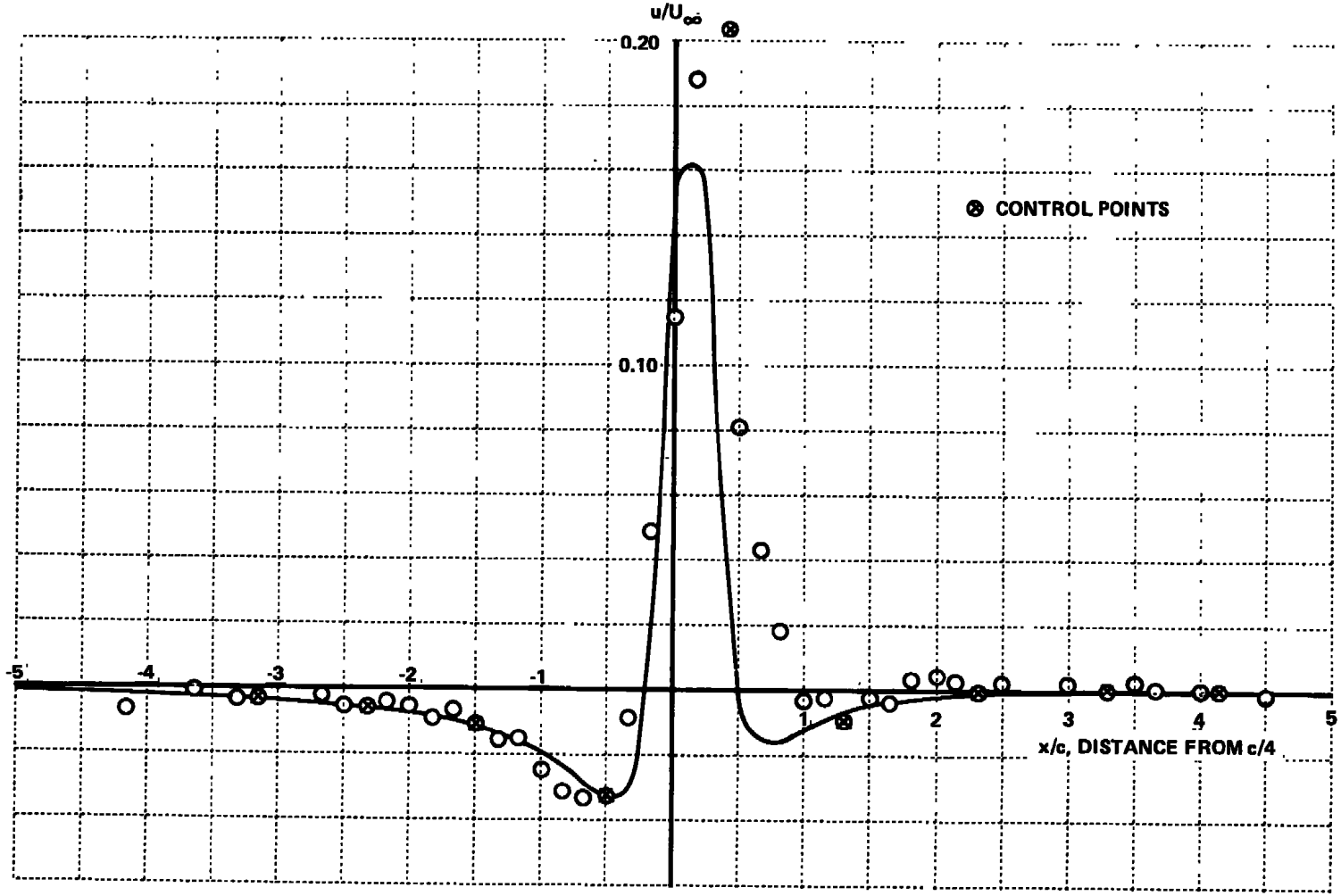

Figure 21 LONGITUDINAL VELOCITY COMPONENTS AT THE UPPER CONTROL SURFACE, $M_\infty = 0.85$, $\alpha = 1^\circ$, 6% BLOCKAGE. WALL CONTROL USED TO ESTABLISH LONGITUDINAL VELOCITY COMPONENTS

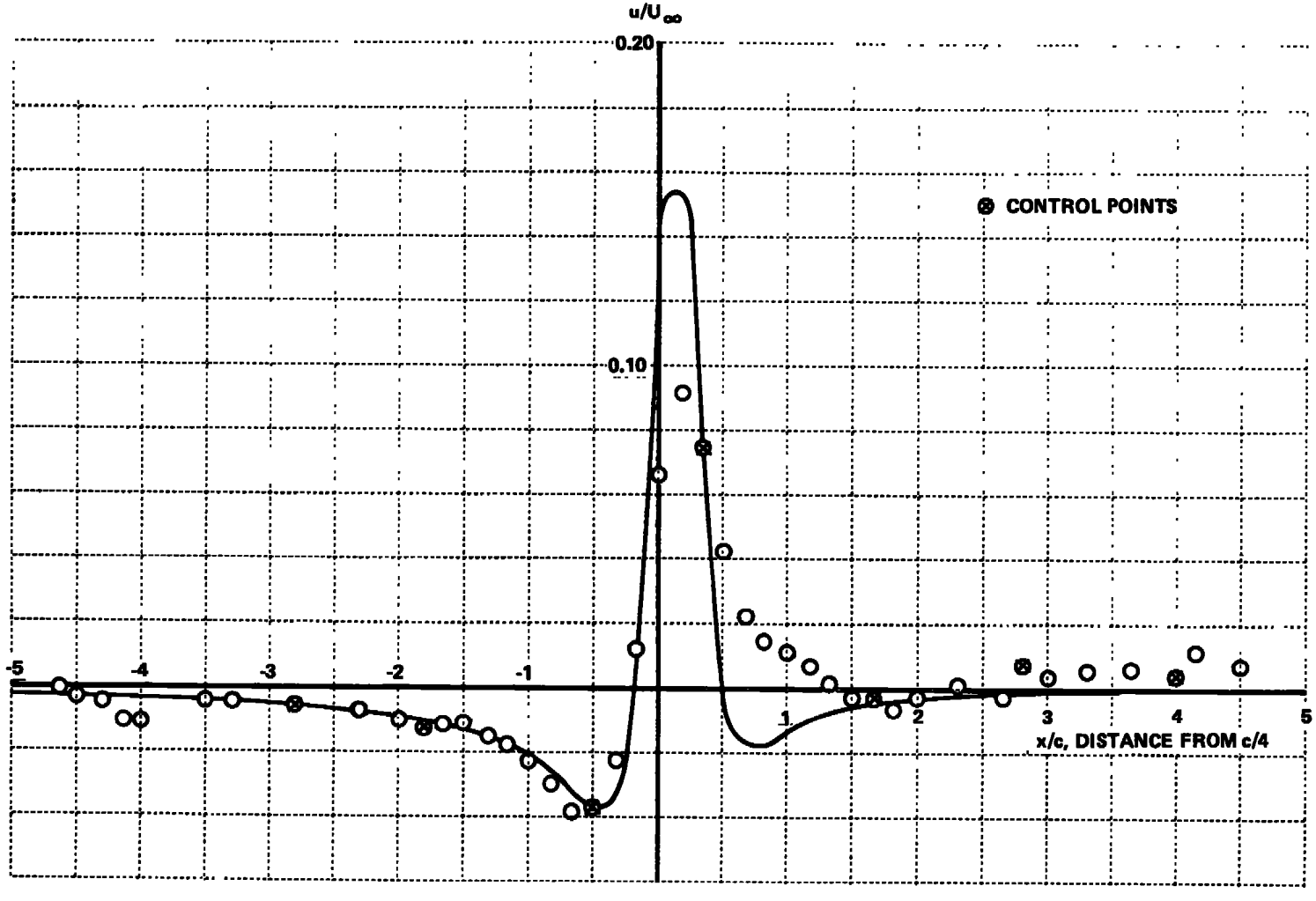

Figure 22 LONGITUDINAL VELOCITY COMPONENTS AT THE LOWER CONTROL SURFACE, $M_\infty = 0.85$, $\alpha = 1^\circ$, 6% BLOCKAGE. WALL CONTROL USED TO ESTABLISH LONGITUDINAL VELOCITY COMPONENTS

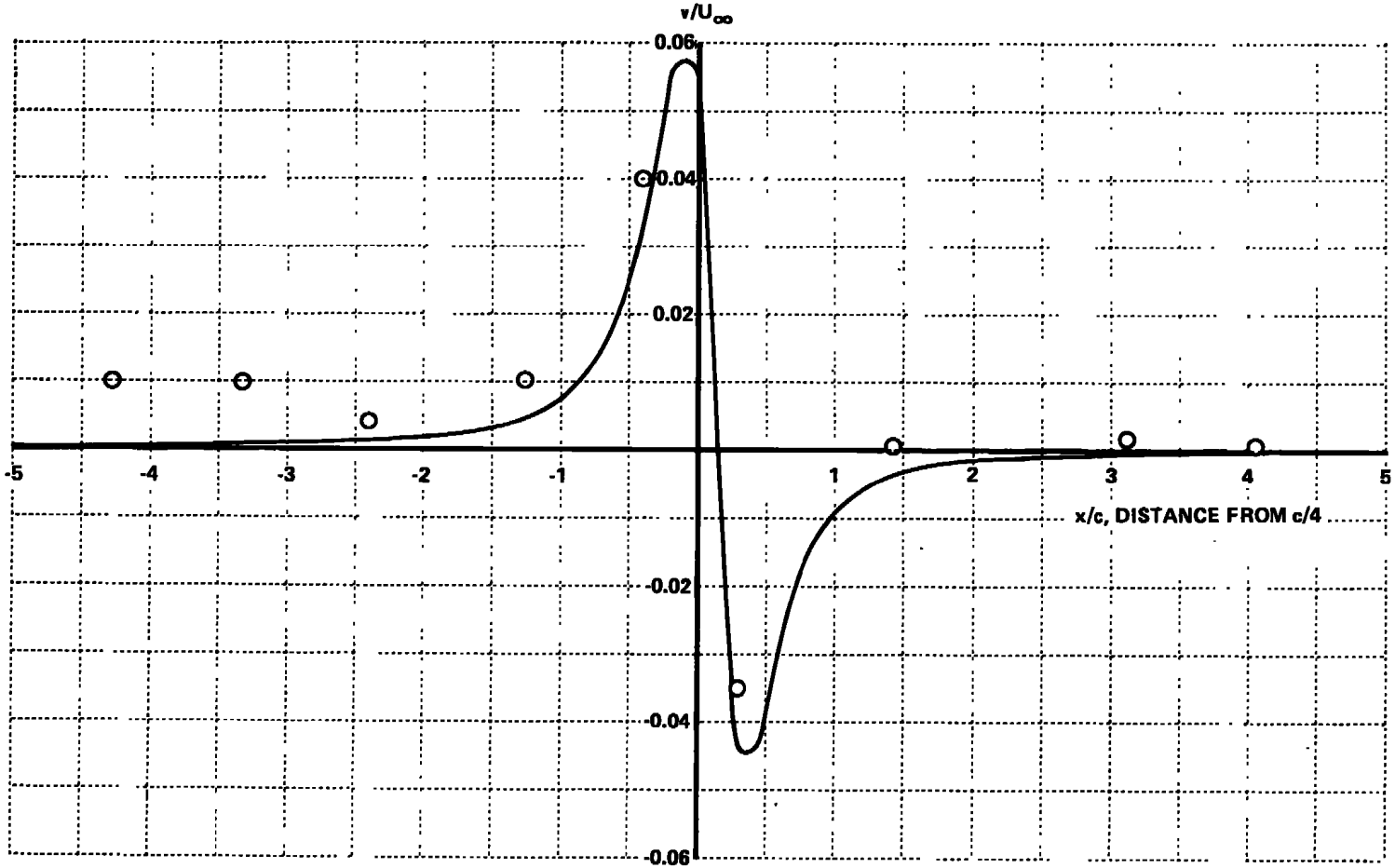

Figure 23 NORMAL VELOCITY COMPONENTS AT THE UPPER CONTROL SURFACE, $M_\infty = 0.85$, $\alpha = 1^o$, 6% BLOCKAGE. WALL CONTROL USED TO ESTABLISH LONGITUDINAL VELOCITY COMPONENTS

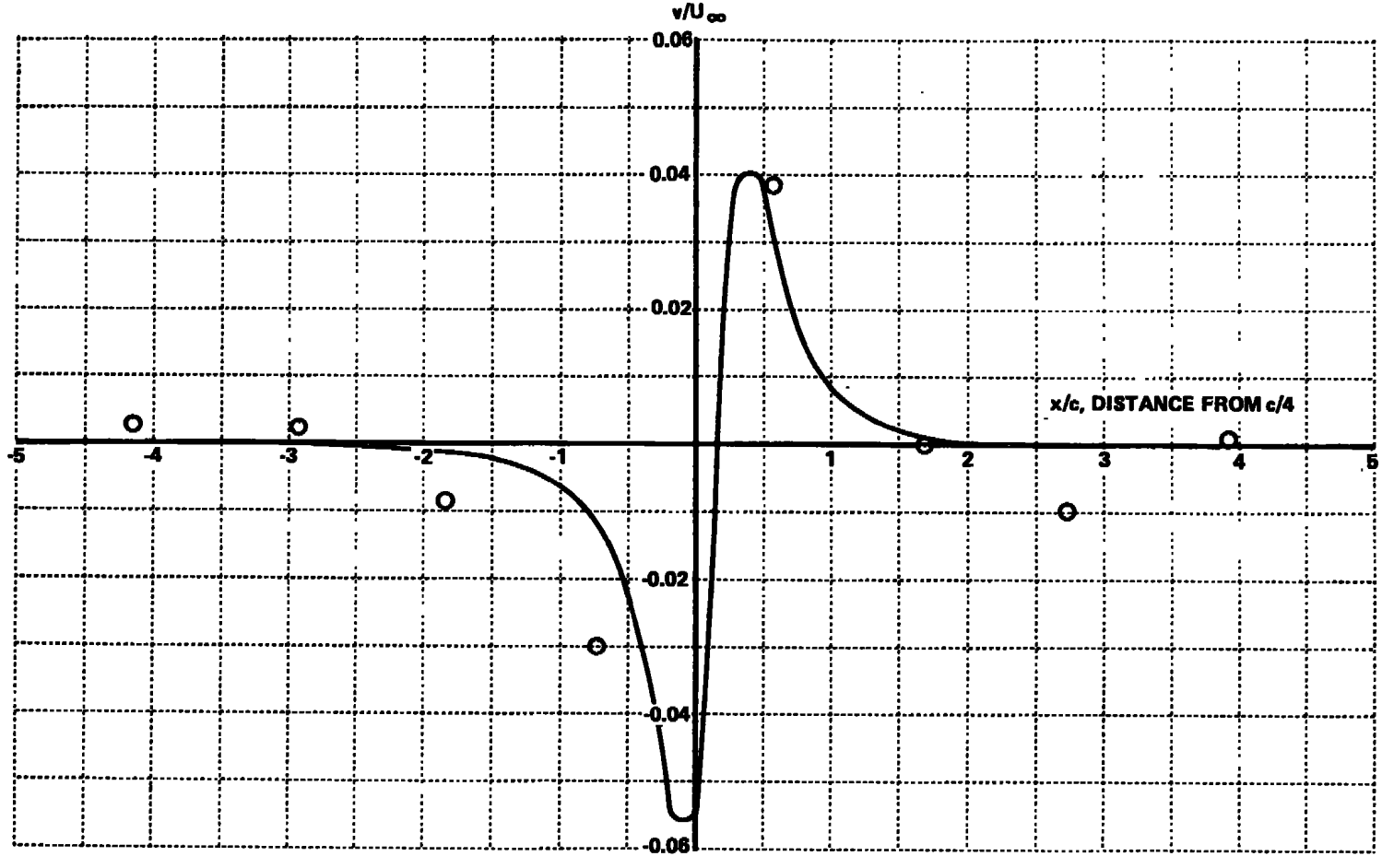

Figure 24 NORMAL VELOCITY COMPONENTS AT THE LOWER CONTROL SURFACE, $M_\infty = 0.85$, $\alpha = 1^o$, 6% BLOCKAGE. WALL CONTROL USED TO ESTABLISH LONGITUDINAL VELOCITY COMPONENTS

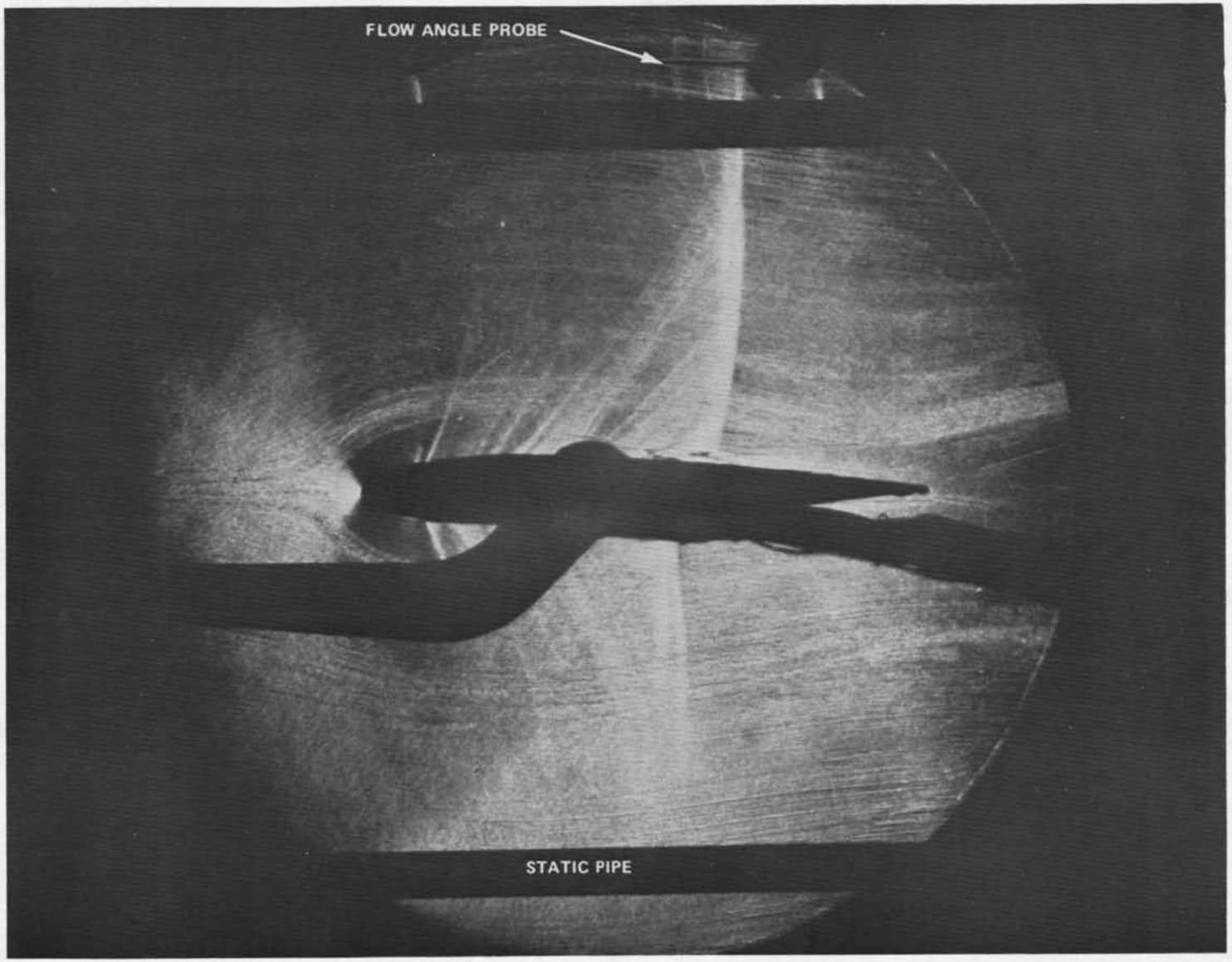

Figure 25 SCHLIEREN VIEW OF THE FLOW FIELD AT $M_\infty = 0.85$, $\alpha = 1^o$, 6% BLOCKAGE. WALL CONTROL USED TO ESTABLISH LONGITUDINAL VELOCITY COMPONENTS

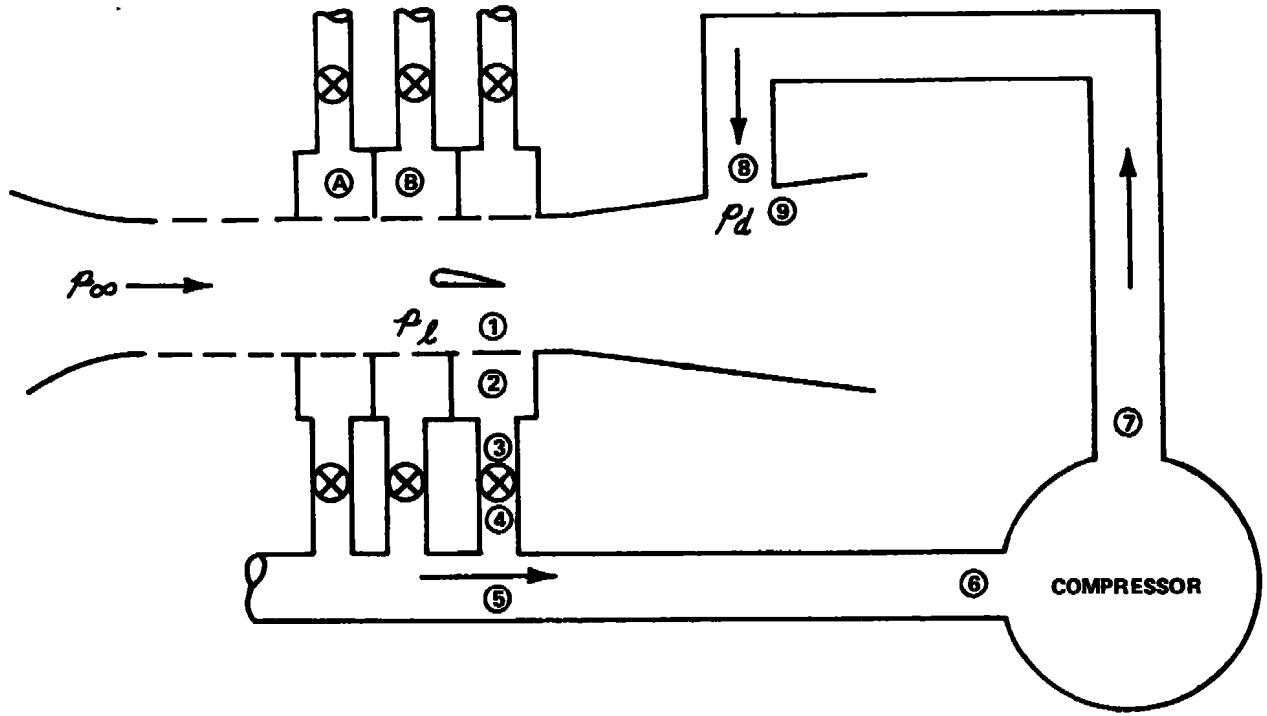

Figure 26 SCHEMATIC OF AUXILIARY COMPRESSOR CIRCUIT

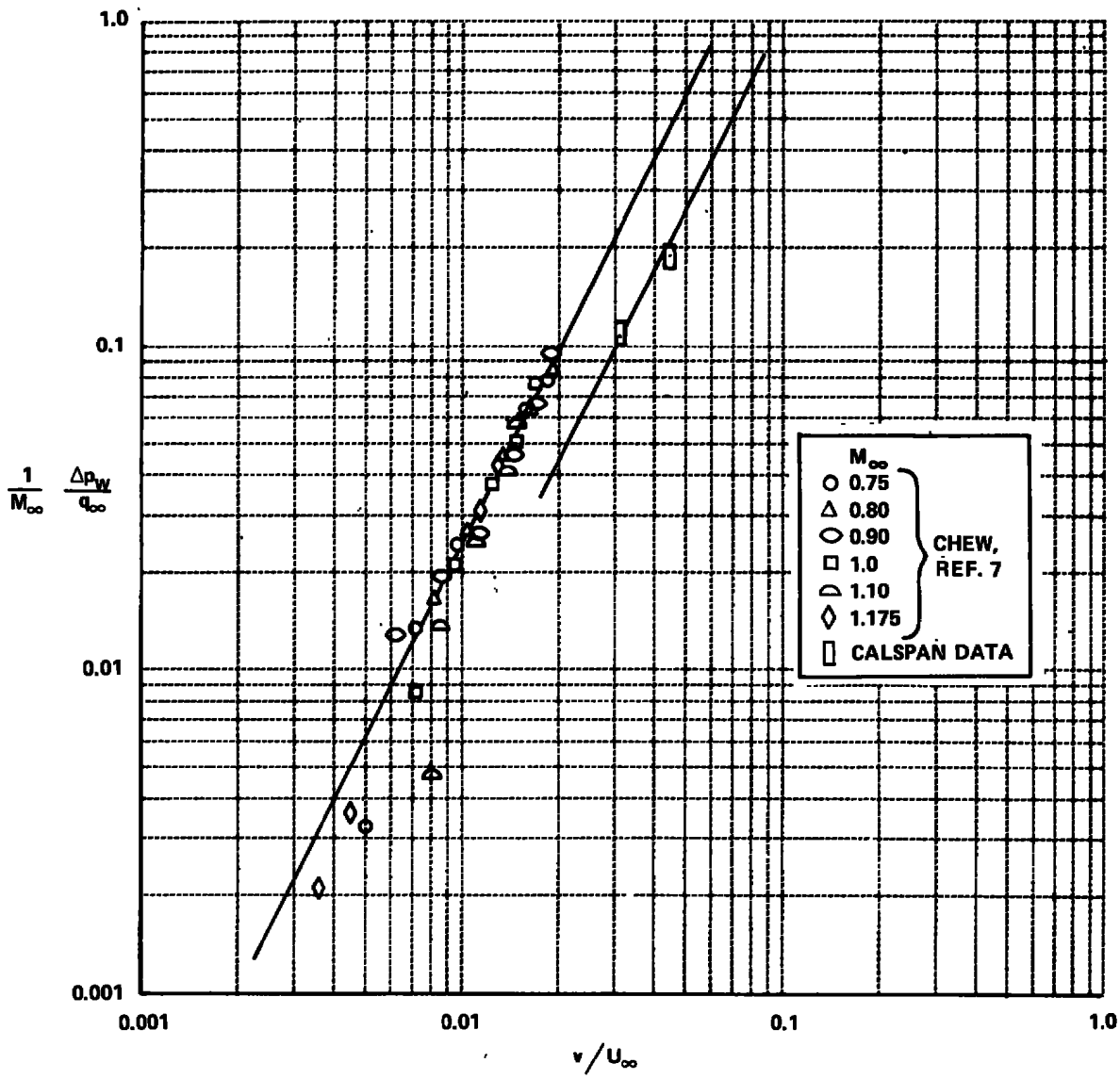

Figure 27 CORRELATION OF LOSS DATA FOR POROUS WALLS – 22.5% POROSITY

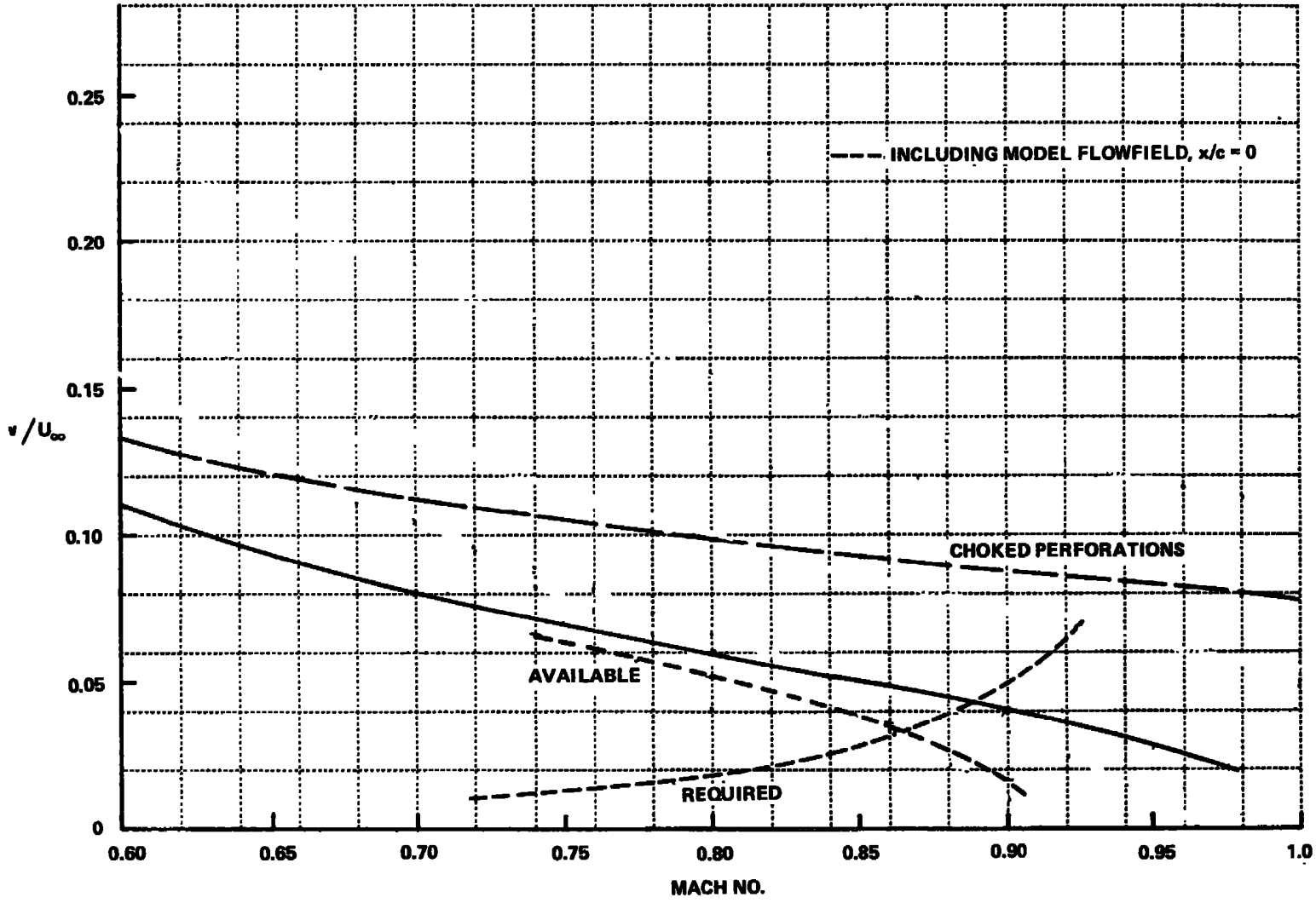

Figure 28 PERFORMANCE OF ORIGINAL AUXILIARY COMPRESSOR CIRCUIT, R_c = 1.43, σ = 22.5%

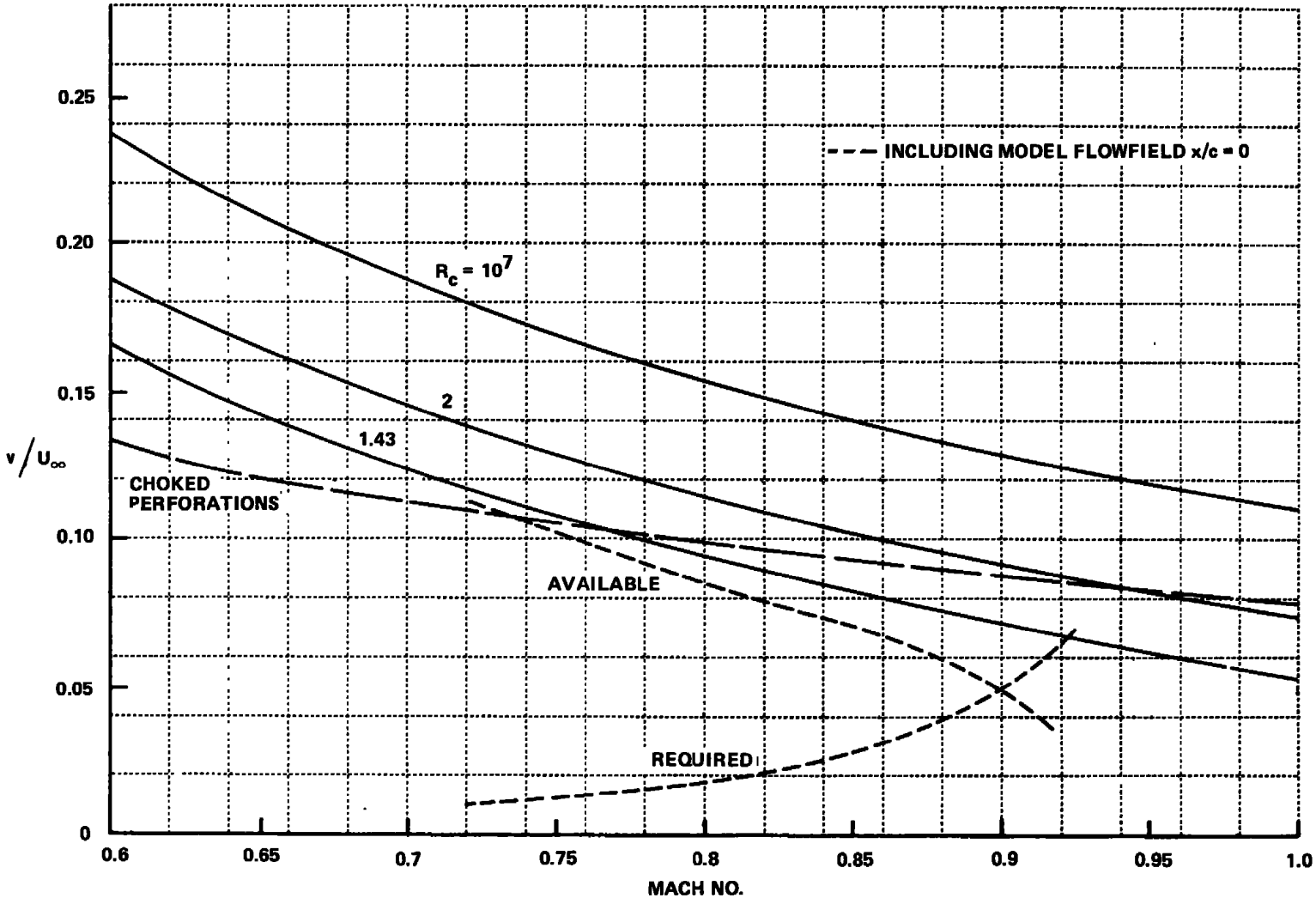

Figure 29 PERFORMANCE OF AUXILIARY COMPRESSOR CIRCUIT WITH SONIC EJECTOR, σ = 22.5%

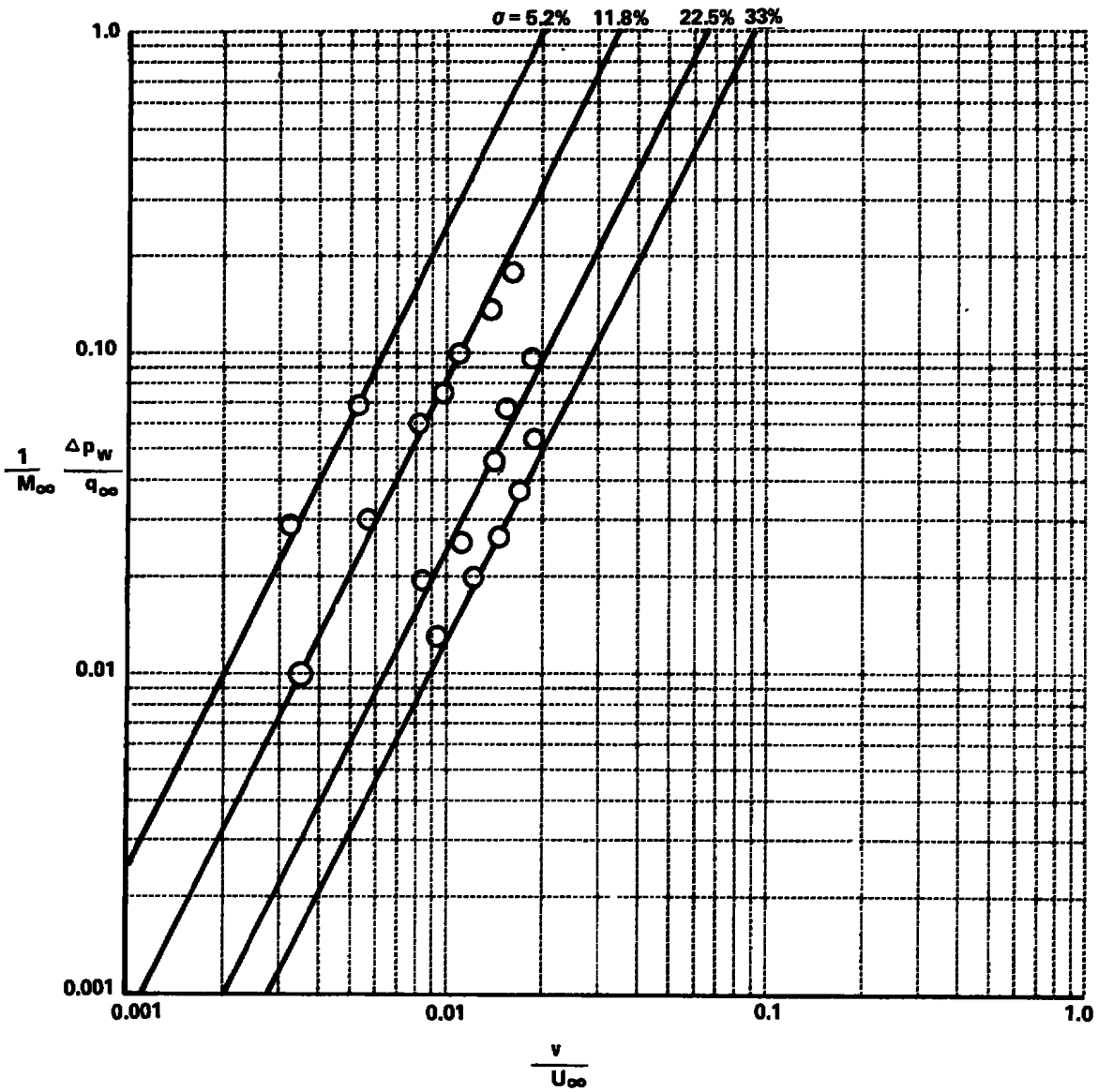

Figure 30 CORRELATION OF REFERENCE 7 DATA FOR POROUS WALLS, $M_\infty = 0.9$

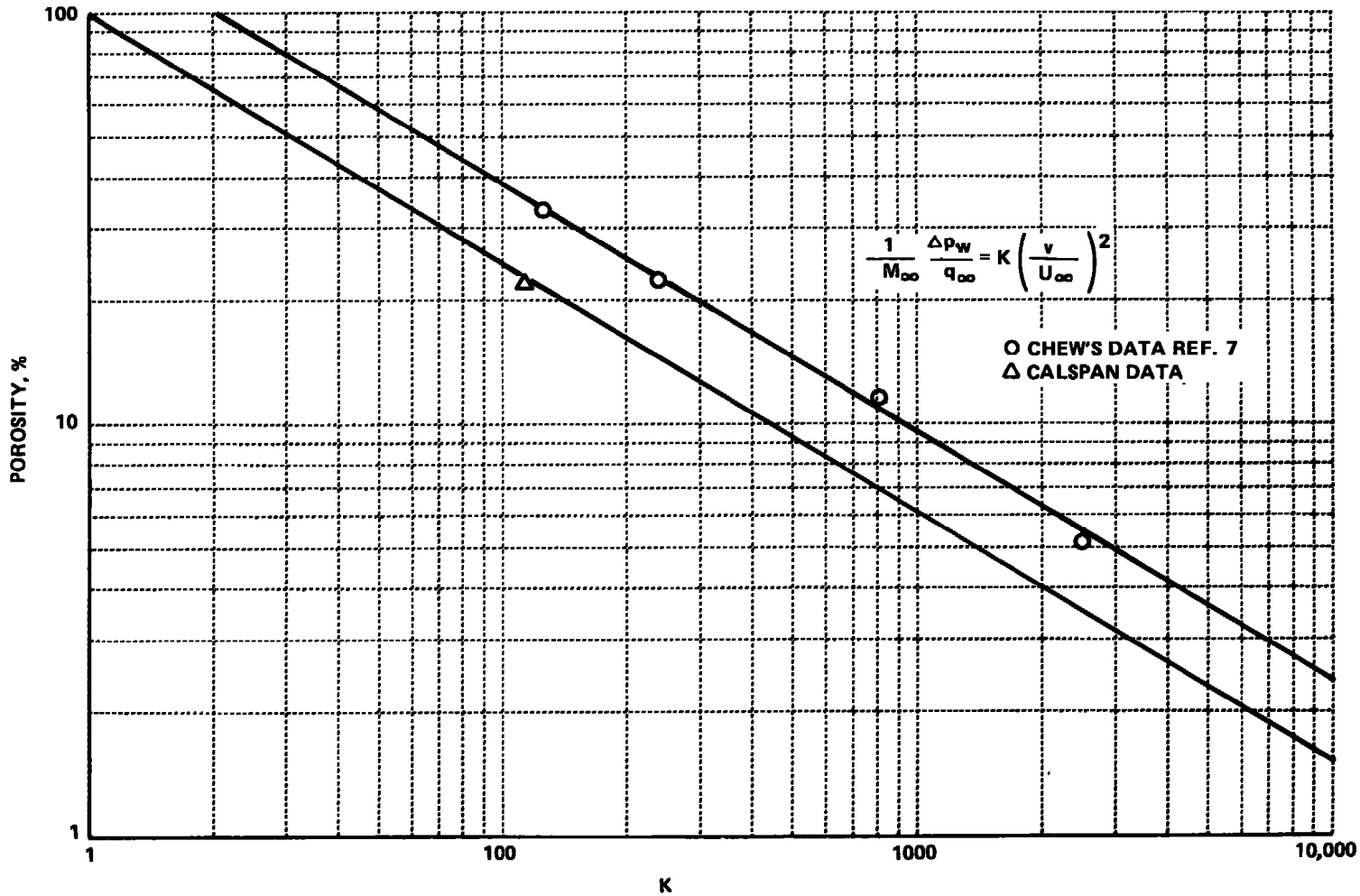

Figure 31 INFLUENCE OF POROSITY ON WALL LOSS CHARACTERISTICS

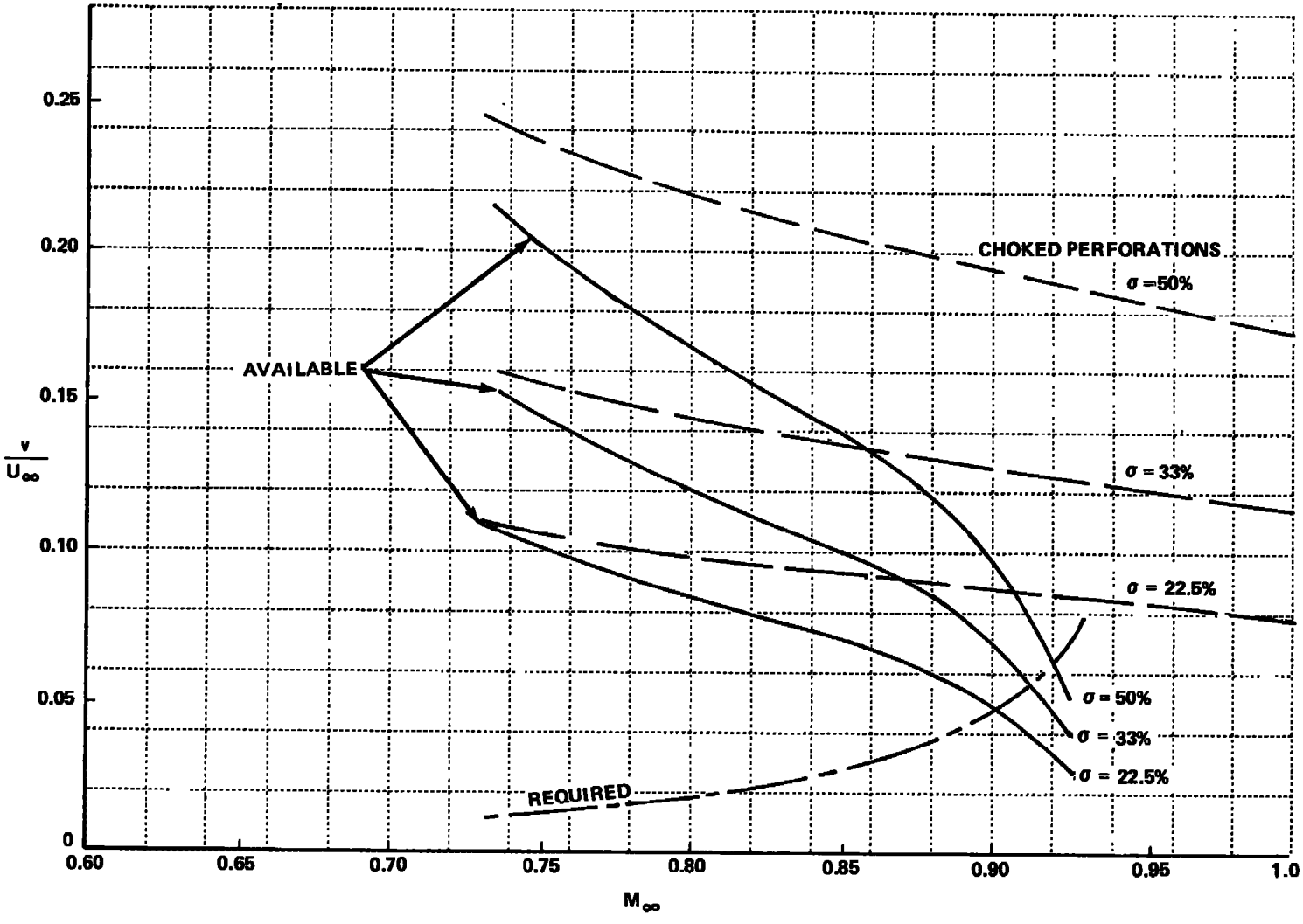

Figure 32 INFLUENCE OF WALL POROSITY ON TUNNEL PERFORMANCE, x/c = 0, R_c = 1.43

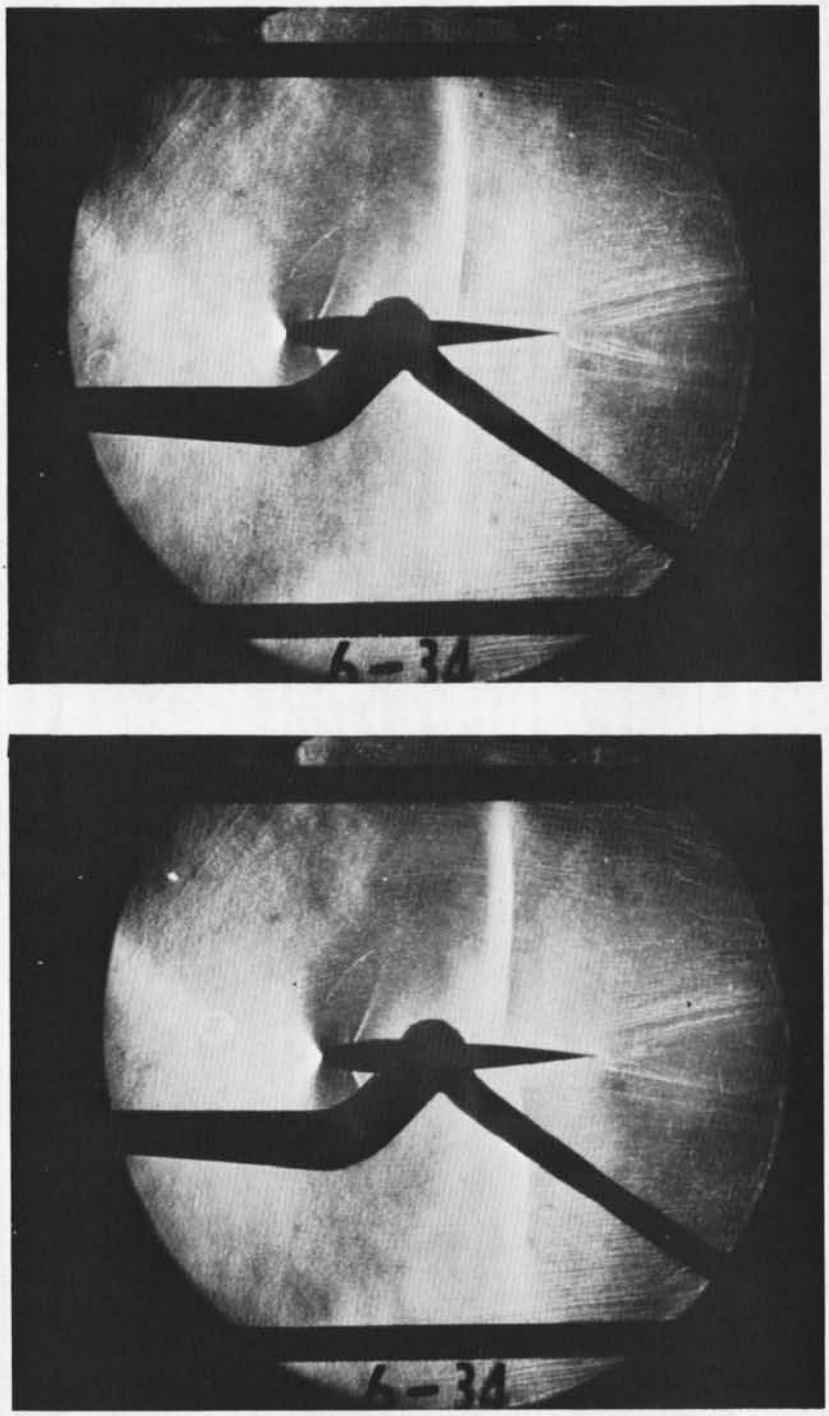

Figure 33 FLUCTUATING SHOCK POSITIONS AT $M_\infty = 0.85, \alpha = 1^o$, 4% BLOCKAGE.